Low-Data Investigation of Higgs Boson Discovery at the LHC

by

Cheyne M. Scoby

A dissertation submitted in partial satisfaction of the
requirements for the degree of
Bachelor of Science

in

Physics

in the

COLLEGE OF LETTERS AND SCIENCES
of the
UNIVERSITY OF CALIFORNIA, SANTA BARBARA

Committee in charge:
Professor David Stuart, Advisor
Professor Deborah Fygenson

Spring 2006

The dissertation of Cheyne M. Scoby is approved:

Advisor Date

Date

University of California, Santa Barbara

Spring 2006

Low-Data Investigation of Higgs Boson Discovery at the LHC

Copyright 2006

by

Cheyne M. Scoby

Abstract

Low-Data Investigation of Higgs Boson Discovery at the LHC

by

Cheyne M. Scoby

Bachelor of Science in Physics

University of California, Santa Barbara

Professor David Stuart, Advisor

The Standard Model (SM) remains as a complete and effective tool for understanding fundamental particles and their interactions. There is only one particle that the model predicts that has not yet been discovered. The Higgs boson is required as part of the mechanism behind electroweak symmetry breaking, and explains how the weak vector bosons, as well as the charged quarks and leptons gain mass, proportional to their coupling to the Higgs field. The SM predicts many properties of the Higgs, but cannot give a precise value to its mass. Experiment and theoretical arguments have put limits on the Higgs mass to within 114.7 GeV/c^2 < M_H < 1000 GeV/c^2. The Large Hadron Collider at CERN will provide access to a new energy regime that will offer many channels for a potential discovery of the Higgs. In the Compact Muon Solenoid (CMS) detector experiment, the "Golden mode" for Higgs discovery features decay to two Z^0, with both Z^0 decaying to leptonic final states. Full reconstruction analyses suffer from the need for a large data set. Here, an

attempt is made to explore analyses of Higgs decay kinematics that may be more sensitive to the Higgs signal, especially for a low-mass Higgs. Since CMS data does not yet exist, analysis of this process must rely on Monte Carlo generated events. The traditional analysis is to find a signal for the Higgs by fully reconstructing the two-Z^0 mass. The analysis presented here will focus on $H \rightarrow Z^0 Z^0 \rightarrow \ell\bar{\ell}\ell'\bar{\ell}'$, and will develop a kinematical signature for this production channel for Z^0 detected from events collected in an integrated luminosity of 1 fb^{-1}.

To my mother,

Wendy,

for giving me the opportunity to be here today, in every possible way.

Contents

List of Figures **iii**

List of Tables **iv**

1 Introduction **1**
1.1 The Higgs Boson 3
1.2 The Large Hadron Collider 8
1.3 The Compact Muon Solenoid 11

2 PYTHIA and Monte Carlo Event Generation **18**

3 Analysis and Discussion **25**
3.1 Full reconstruction 26
3.2 Transverse Momentum Signature of a Single Z 32
3.3 Transverse Momentum of a Z with a Third Lepton 32
3.4 Kinematics of a Trilepton System 37

4 Conclusion **43**

Bibliography **47**

A PYTHIA code **48**

B A typical PYTHIA event dump **52**

List of Figures

1.1 Feynman diagrams for Higgs production subprocesses 5
1.2 Cross sections for pp→H production subprocesses 6
1.3 Branching ratios for H→XX decay channels. 7
1.4 LHC tunnel photograph 8
1.5 Artist's rendition of the LHC 9
1.6 Map of the LHC 10
1.7 Expanded and labelled diagram of the CMS detector 12
1.8 Transverse slice through the CMS detector 13
1.9 Simulated Higgs decay in the CMS tracker 14
1.10 ECAL energy resolution 17

2.1 PDF for a proton at the LHC 19
2.2 PYTHIA-calculated Higgs production cross sections at the LHC 23
2.3 PYTHIA-calculated Higgs branching ratios 24

3.1 Full reconstruction of the Higgs from four leptons 27
3.2 Invariant mass plots of the Higgs candidates 28
3.3 Significance plot for full reconstruction 30
3.4 A tally of the number of leptons per signal event 31
3.5 Reconstruction of a single Z 33
3.6 Transverse momentum plot for a single Z 34
3.7 A tally of the number of leptons per event 35
3.8 p_T for Single Z (plus lepton) 36
3.9 Significance plot for p_T(Z) (with an extra lepton) 37
3.10 Partial reconstruction of the trilepton 38
3.11 Histogram of the trilepton mass 39
3.12 Significance plot for the trilepton mass 40
3.13 Histogram of the trilepton transverse momentum 41
3.14 Significance plot for the trilepton transverse momentum 42

4.1 Significance for all analyses 44
4.2 Projected significance for HIggs discovery 45

List of Tables

2.1 Summary of leading-order Higgs production PYTHIA subprocesses 20
2.2 Summary of Z background-producing PYTHIA subprocesses. 20
2.3 PYTHIA-calculated cross sections for Higgs and SM Z production at the LHC 22

Acknowledgments

I would like to thank the support and encouragement of my advisor, D. Stuart; without his weekly meetings and pep talks I would probably still be trying to figure out how to turn on my computer. I owe much of my experience as a scientist to E.G. Gwinn who gave me my first stand in the trenches and who always provided a friendly conversation. Additional gratitude to my students at CLAS as well as to my colleagues in the UCSB physics department for listening to my ramblings about "quarks and such." Finally, to my entire family, for their love and support, and for not worrying too much when I failed to call home for a few months.

Chapter 1

Introduction

Particle physics is the study of the tiniest, indivisible, fundamental constituents of the universe. Through decades of experiment and inspired theoretical leaps, physicists have developed a working theory of matter and its interactions. The standard model (SM) of particle physics stands as a usable theory of what particles should exist, how they should decay and be produced, and how they must interact with one another. SM physics has been well-tested by numerous experiments, and so far every observation made has agreed with the results this model predicts. Its strength as a description of the universe leads physicists in a search for the last undiscovered particle predicted by the SM - the Higgs boson.

The Higgs mechanism is responsible for electroweak symmetry breaking. It explains why, at normal distances and energies, the electromagnetic and weak forces are not unified. Furthermore, through the strength of its coupling to other particles, it describes why weak vector bosons (Z^0, $W^{+/-}$) are massive, while the photon (γ) gains no mass since it cannot interact with the Higgs field. Therefore, the masses of particles serve to identify

the relative magnitudes of the strength of their couplings to the Higgs field. The mass and the coupling strengths of the Higgs boson have thus far prevented its observation.

Although theory[2] has predicted that the mass of the Higgs boson must be less than 1 TeV without requiring a revision of the standard model, a further calculation of an exact value of the Higgs mass, M_H, is not possible. Searches[3, 5] in various colliding beam experiments, such as those conducted at the Large Electron-Positron collider (LEP) at the laboratory of the *Conseil Européen pour la Recherche Nucléare* (CERN) in Geneva, Switzerland, as well as those conducted at the Tevatron at Fermi National Accelerator Laboratory (Fermilab) in Batavia, IL, USA have not turned up conclusive evidence for existence of the Higgs. As far as theory and experiment predict, if the standard model is self-consistent, the Higgs mass could lie anywhere between 115 GeV/c^2 and 1000 GeV/c^2.

Further searches for the Higgs will continue as the D0 and CDF experiments at Fermilab gather more data. At present collision rates (*luminosity*), the Tevatron is not likely to provide enough data to make a convincing argument for the discovery of a low-mass Higgs before the end of its current run. Likely, the problem of producing Higgs at a high rate must be addressed by running collider experiments at higher energies and luminosity than this accelerator can provide.

The answer is provided by a new accelerator machine currently under construction at CERN. The Large Hadron Collider (LHC) is an international collaboration to produce the most advanced particle accelerator in the world. It is expected to run at a center-of-mass energy of $\sqrt{s} = 14$ TeV. This is more than seven times the center-of-mass energy of the Tevatron, which has thus far claimed the high energy record.

Understandably, there is much interest in finding the Higgs and fully validating the SM. This, coupled with the sheer size of the collaboration, motivates the effort of many researchers who hope to find the Higgs. In hopes of finding a high-mass Higgs, many other researchers are trying to reconstruct the Higgs fully from its decay to four leptons, the so-called "Golden mode" for Higgs discovery at the one of the detectors at the LHC, the Compact Muon Solenoid experiment.

However, full reconstruction requires a lot of data. By considering other kinematics of Higgs decay at the LHC, the analysis presented here will explore an interesting and unique method of searching for the Higgs, that could provide increased sensitivity, especially with a small, initial data set.

Before starting on the analysis described above, it is useful to learn a little about the Standard Model Higgs boson, the Large Hadron Collider, the Compact Muon Solenoid, and about Monte Carlo simulations in particle physics.

1.1 The Higgs Boson

Particle physics is built on principles of symmetry in the universe, yet the masses of the SM fundamental particles are indescribable by any current theory. Even more interesting are the weak vector bosons, the $W^{+/-}$ and Z^0. At high enough energies, the weak and the electromagnetic interactions unify. Therefore, the weak carriers, the W and Z, should be on equal footing with the carrier of the EM interaction, the photon. However, as the two forces condense and separate at lower energies, the W and Z gain mass, while the photon remains massless. The answer is that the universe seeks a lower energy, spontaneously breaking the

symmetry. The mechanism responsible for the spontaneous electroweak symmetry breaking requires particles to interact with a scalar *Higgs* field. The theory[1] further predicts the existence of a massive scalar boson, the Higgs particle, which serves as the mediator between this field and other particles. Through this mechanism, the other particles obtain a mass proportional to the strength of their coupling to this field, explaining why the charged leptons and the weak vector bosons are massive.

Because of its important place in the SM, experiments have searched for the Higgs for more than three decades. Primarily collider detector experiments at the Tevatron at Fermilab and the LEP collider at CERN have searched unsuccessfully for a Higgs signal. However, these experiments have been able to set limits on the range of the Higgs mass. They exclude a Higgs mass less than 114.7 GeV/c^2. If the mass were less, these experiments would have found evidence for a signal. Furthermore, these experiments have provided an extensive body of electroweak data. Various fits to this data have also suggested that the Higgs mass should be at the low end of this range, less than 200 GeV/c^2, which is just out of reach of currently running accelerators. Though the theory identifies many properties of the Higgs, it cannot provide a more precise value for the mass of the Higgs particle.

There are several production modes for the Higgs particle from a hadron collider. A hadron is basically a bound state of quarks, held together by the strong-force carrying gluons. Thus, in a hadron collision, these quarks and gluons interact to produce the Higgs. The Higgs can only couple to massive particles, and so the massless gluons can only interact through loop diagrams with top and bottom quarks that can then couple to the Higgs. Figure 1.1 shows the five leading contributing subprocesses to Higgs production in a hadron

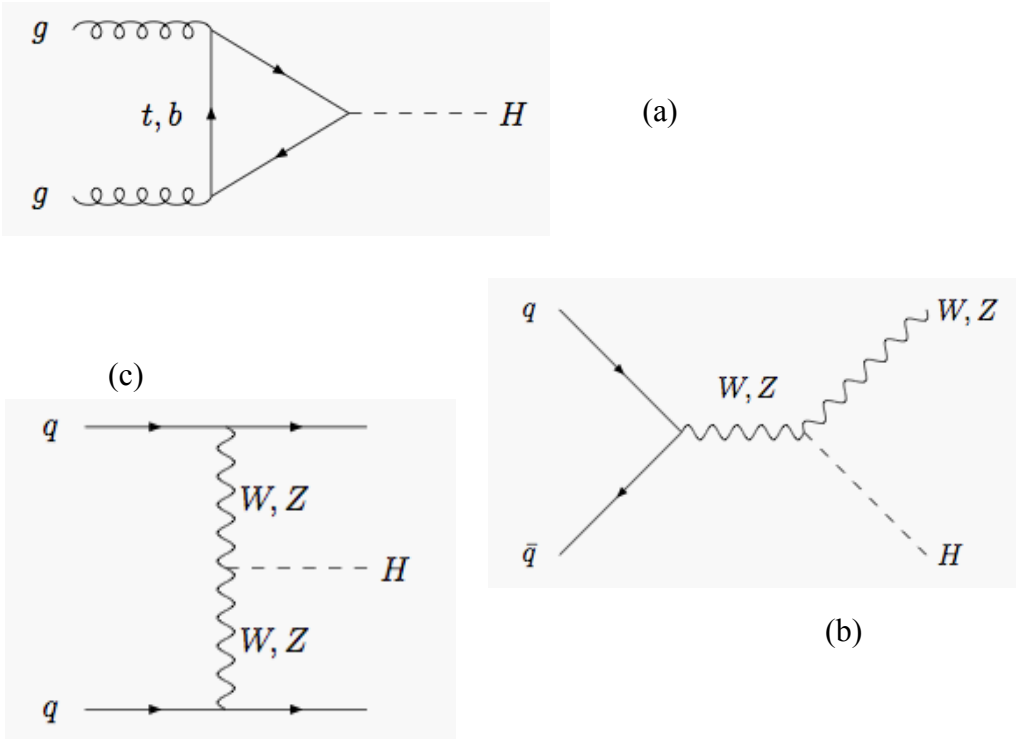


Figure 1.1: Feynman diagrams for the top five Higgs production subprocesses. (a) gluon fusion, (b) neutral and charged higgsstrahlung, (c) neutral and charged weak vector boson fusion.

collider.

The effective production rates (*cross sections*) for the Higgs at the LHC are derived through a quantum field theoretical calculation of a *matrix element*. The matrix element is obtained by summing the quantum mechanical amplitudes of all the production subprocesses shown in the Feynman diagrams in Figure 1.1. To be complete, this sum must include an infinite number of higher-order diagrams containing loops and initial state radiation. However, in practice the sum is truncated to leading order (LO) or next-to-leading order (NLO) diagrams in a perturbative expansion. This matrix element is then integrated over

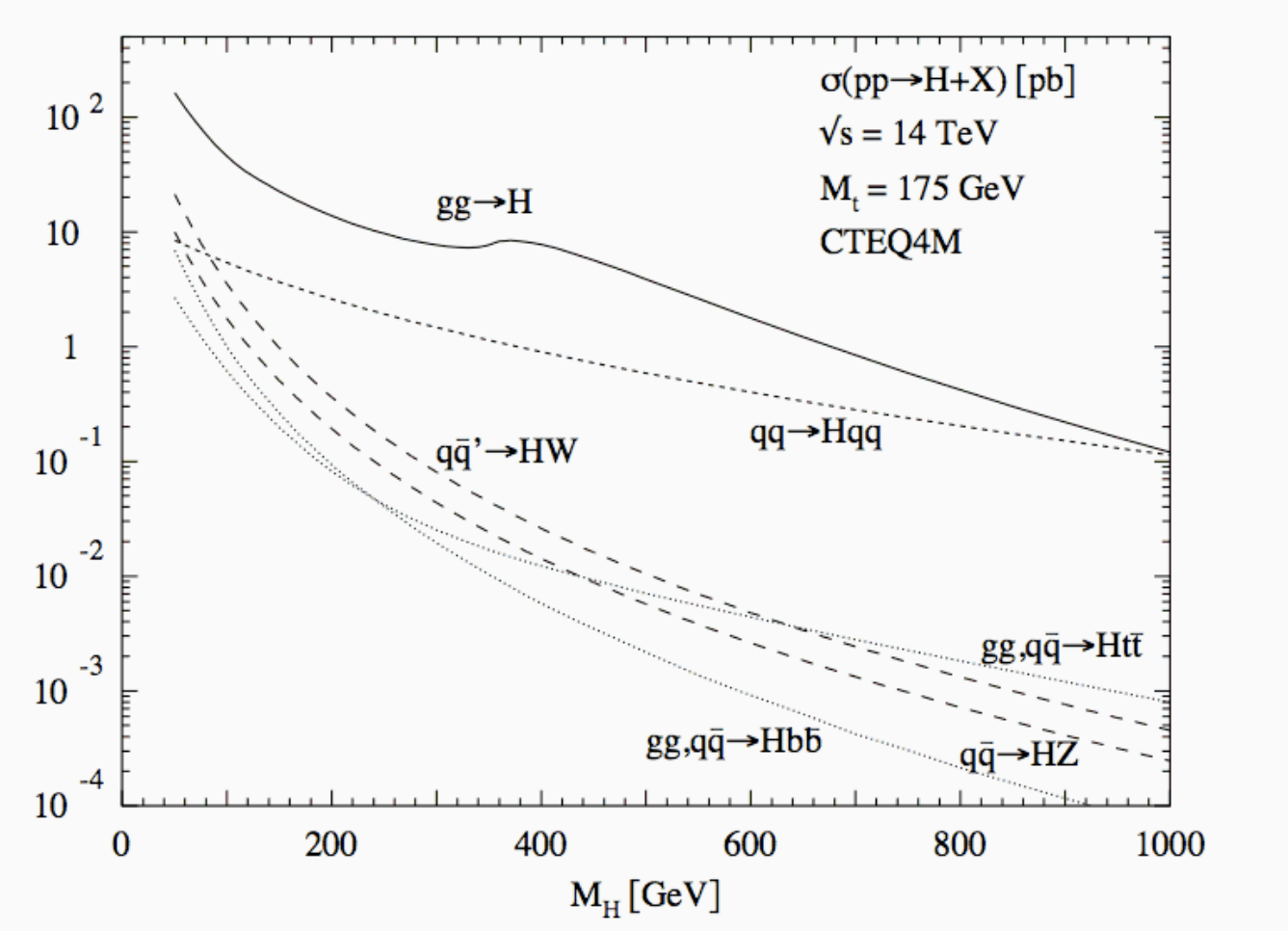


Figure 1.2: NLO calculation of total cross sections for pp→H production subprocesses.

the phase-space, and thus depends on the initial-state momenta of the collided particles as well as the Higgs mass. Figure 1.2 shows the result of a NLO calculation[2] giving the total cross section for the leading Higgs production subprocesses as a function of Higgs mass. Once the cross section is calculated the number of Higgs produced for a given data set can be calculated; $N_{prod.} = \sigma \times \int L\,dt$ where L is the *luminosity* (related to the collision rate) of the collider.

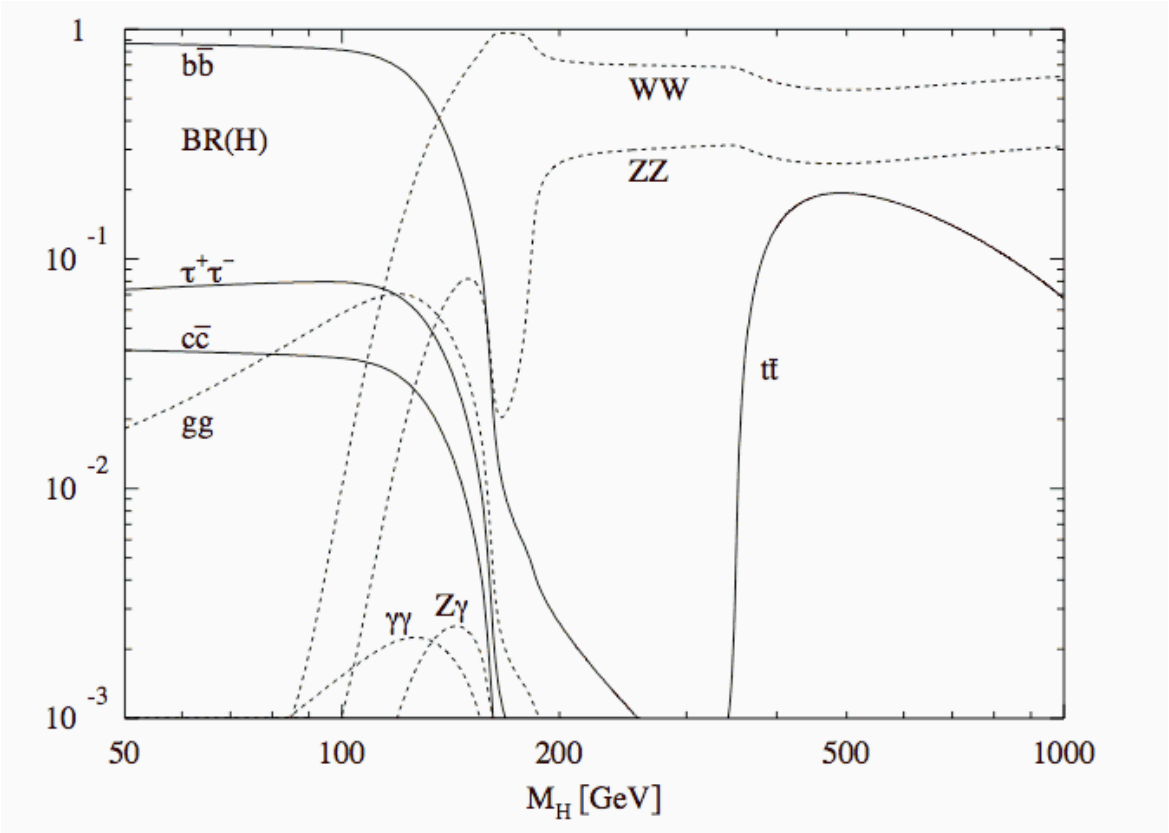


Figure 1.3: NLO calculation of branching ratios for Higgs decay channels.

Because of its mass and ability to couple to lighter particles, the Higgs boson is unstable. Once it is created it can decay through any of several decay channels. The decays are random, and each mode can be associated with a probabilistic decay rate in terms of the fractional rate for the particle to decay through a specific channel. This fraction is called the *branching ratio*. Like the cross section, these ratios can be calculated by considering Feynman diagrams for H $\rightarrow$ XX. Again, the calculation depends on the mass of the Higgs, which is taken as a variable in an NLO calculation[2] that is shown in Figure 1.3.

At these rates, the LHC will be capable of producing an appreciable number of



Figure 1.4: The excavated and bare LHC tunnel.

Higgs bosons. The machinery that is being put into place at CERN to produce and detect this particle is mind-boggling.

1.2 The Large Hadron Collider

The Large Hadron Collider (LHC) is a new particle accelerator under construction at the laboratory of the CERN laboratories in Geneva, Switzerland, set to open in June 2007. The machine is a synchrotron designed to accelerate protons to very high speeds in highly coherent beams. The two beampipes will circulate protons in opposite directions, and the beams will be squeezed to cross at two locations along the ring's circumference, known as the interaction points. At these speeds, the proton-proton system will gain a center-of-mass energy of $\sqrt{s} = 14$ TeV. This energy will break the record, currently held by the Tevatron at Fermi National Accelerator Laboratory in Batavia, IL at $\sqrt{s} = 1.96$ TeV.

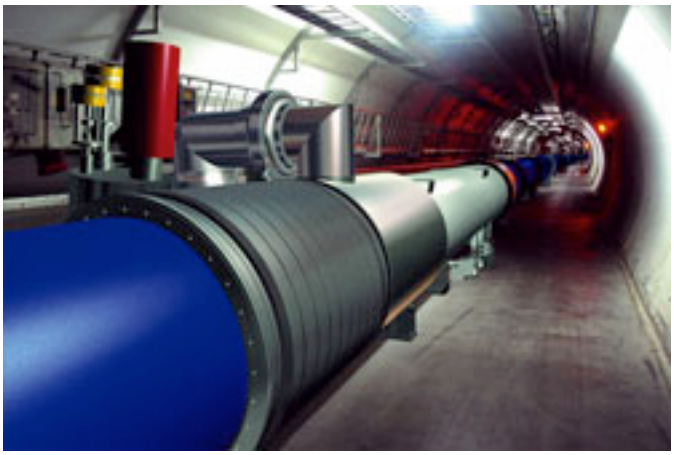
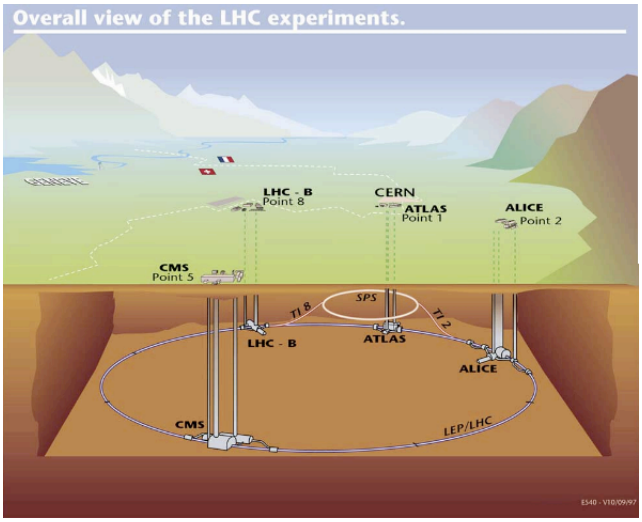


Figure 1.5: An artist's rendition of the complete LHC tunnel.

This increase in energy is not trivial for at least two reasons; Firstly, as discussed, the almost order-of-magnitude increase will make the Higgs boson discovery possible, even if its mass lies at the 1 TeV theoretical upper limit. Secondly, the accelerator will be of much larger scale than any project ever completed. The ring will undercut the French and Swiss countryside for a total diameter of 27 km at depths spanning 50 m to 150 m . An overhead view of CERN and the LHC is drawn in Figure 1.6.

The engineering required for a project of this scale is unlike anything every attempted in the history of particle physics. The most recent estimates for the cost of completing the LHC is several billion dollars. The LHC was able to take advantage of the preexisting tunnel, constructed for the LEP, which is now decommissioned. The majority of the cost arises from the 1232 superconducting dipole magnets that will line the entire ring. Each magnet is 15 m long, weighs 35 tons, and requires a constant supply of liquid helium to operate in its intended superconducting state.



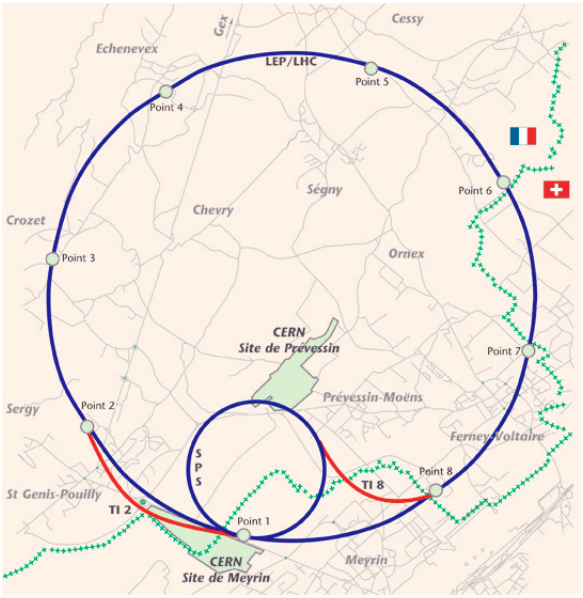


Figure 1.6: A map of the 27 km diameter LHC, spanning two countries at a depth of 100 m. CMS sits at Point 5. Maps taken from CERN's LHC website.

This accelerator has stretched the limits of engineering and the minds of scientists around the world. As a result, it should be able to produce Higgs bosons in copious quantities. However, producing them is no good without the ability to measure them.

1.3 The Compact Muon Solenoid

The Compact Muon Solenoid is the detector used in one of two experiments that will record events in the highest energy collisions at the LHC. The detector is being built by the CMS collaboration, which is composed of more than 160 universities and laboratories in 36 countries all over the world. The name of this detector outlines its three salient features.

Although it does not pass the traditional "smaller than a bread box" classification, the active percentage of CMS is much higher than any detector rightly giving it the name "compact." Built from layer after cylindrical layer wrapped around the LHC beampipe, the detector branches out to a diameter of 15.0 m. The distance between either end in the direction along the beampipe is 21.5 m. With the tight packing of steel, scintillator, and silicon, it weighs in at 1.25×10^8 kg. Below, Figure 1.7 shows an expanded view of the detector, labelling some of the components critical to detecting all different types of particles that collisions will produce.

Muon detection is the middle name of this detector. The muon detecting chambers comprise the outer layer of this jelly-roll detector. This portion has been engineered to detect muons, and record their momentum and energy as precisely as possible. This system has made muon detection an integral part of many analyses proposed for CMS physics, including those outlined in this paper.

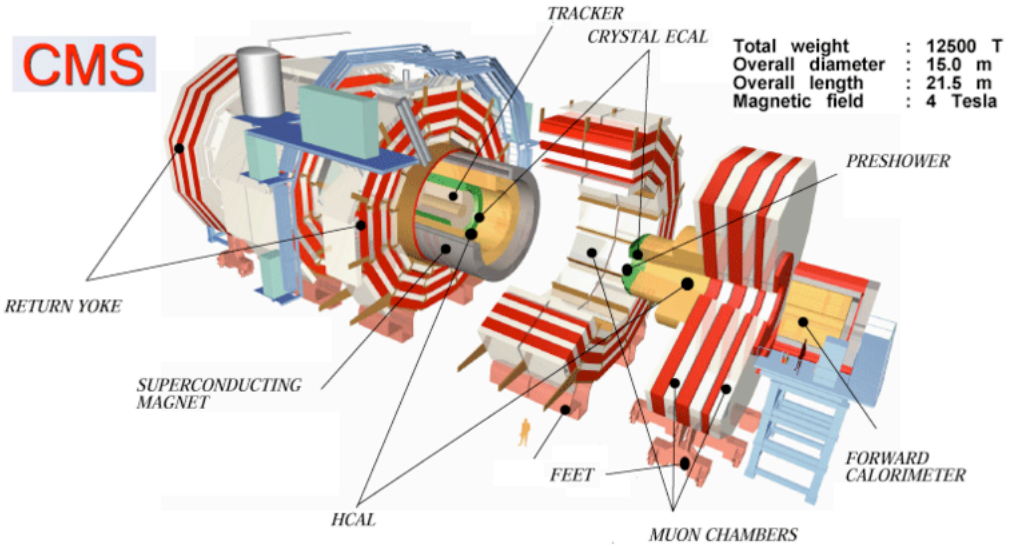


Figure 1.7: An expanded and labelled diagram of the CMS detector.

In order to measure the momentum of charged particles produced in the proton collisions, it is necessary to set up a magnetic field inside the detector. The third part of the name of this detector hints at how the magnetic field is provided. A large solenoid wraps through the layers, setting up a field that bends charged particles as they move away from the beampipe.

The properties of the different parts of the detector allow particles to be identified by how they interact with the different materials. In a rough sense, the detector can be thought of as a cylindrically-layered cake. After a proton-proton collision, the particles produced in the interaction fly outwards in all directions. Figure 1.8 shows a transverse slice of the detector, with a few lines drawn in that are representative of different particles produced in a collision.

The first layer is the silicon vertex tracker. The tracker consists of arrays of sil-

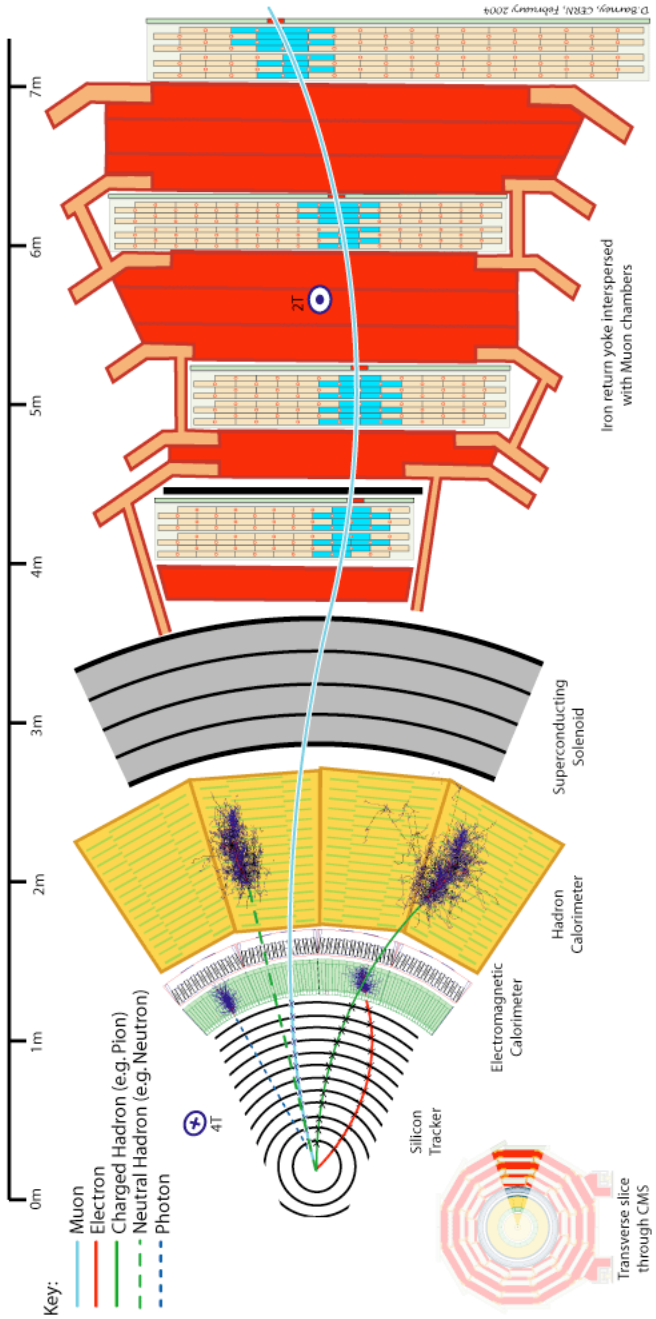


Figure 1.8: A transverse slice through the CMS detector. A few representative particles are drawn to show where they deposit the most energy. Electrons and photons are stopped by the ECAL. Jets penetrate into the HCAL. Muons are energetic enough to punch through to the outer layer of the muon system where their energies are better measured.

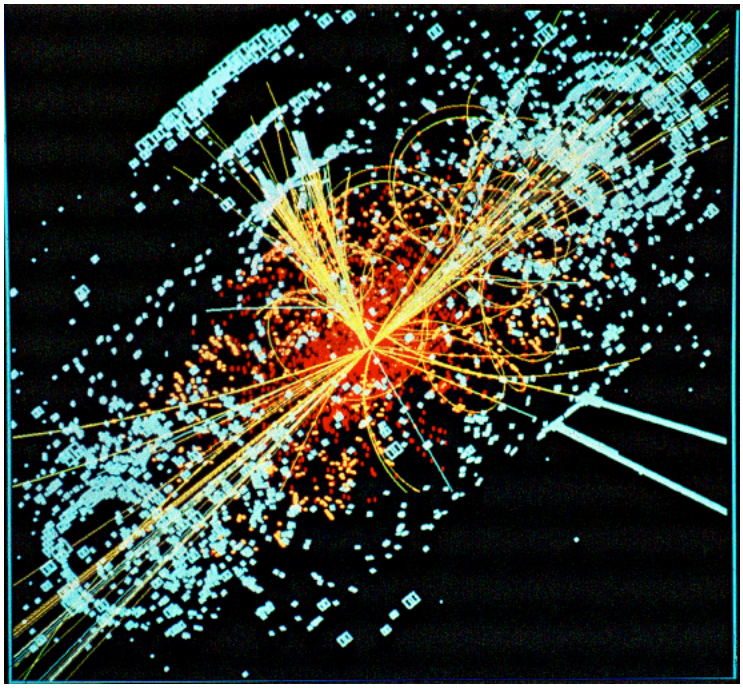


Figure 1.9: The simulated decay of a Higgs particle, as seen by the CMS tracker. The blue stubs show energy deposited in the EM calorimeter

icon strips mounted on holder rods immediately surrounding the beampipe. These rods are tiled into a tightly-packed formation, with a total diameter of 2.4 m, covering a total area of 210 m^2. The endcap sections of the tracker also contain very high resolution silicon pixel detectors. Charged particles passing through the silicon can excite electrons across the material's bandgap, forming electron-hole pairs in the material in an ionization process. As these pairs migrate in the electric field applied across the silicon, they give a recombination current that can be read out and processed into meaningful signals by the readout electronics. This arrangement allows particle positions to be measured to a few tens of micrometers. In this way, there is a reliance on the ability to produce a very uniform and well-understood magnetic field in the tracker region, since the momentum measurement is a direct calculation from this information. Reconstruction and analysis techniques such as B-tagging also rely on the ability to located a decay vertex displaced from the point of the original collision.

The next layer of the detector is the electromagnetic calorimeter (ECAL). It is designed to record the energy of light charged particles (namely electrons) and photons, and stop them from continuing through the detector. This layer is composed of lead tungstate crystals. The material here has the heaviest atoms possible to isolate electromagnetic showering while still being clear enough to allow light pulses to be read out by a solid-state multi-photon detector called an avalanche diode. Thus, only a small part of the ECAL will be blinded by an incoming particle, leaving plenty of the detector ready to observe particles produced in the next collision.

The next layer is the hadron calorimeter (HCAL), designed to measure the energy

of color carrying particles. Essentially, this layer consists of layer after layer of interacting copper and scintillator plates, designed to stop and measure the energy of hadronic showers (jets). These particles experience strong interactions with the nuclei of the HCAL with low scattering.

After the HCAL comes the source of the magnetic field. A large solenoid (the inner diameter is 5.9 m) made out of coiled superconducting wire and is cooled to its superconducting state at 4 K by liquid helium circulation is used to provide the field. In addition to having the nice property that the field is roughly uniform and longitudinal down the beampipe, it is one of two or so geometries that can be calculated using Ampère's law! The setup gives a field of 4 T from the beampipe to the edge of the solenoid. This field strength is carefully chosen to allow good tracking and calorimetry, and is essential to do what the CMS was designed for, identify and trigger on muons.

Much of important CMS analysis of new physics processes is expected to be built on the measurement of high momentum muons. Between the high-precision tracker, and good energy resolution of the muon calorimeter, the efficiency for muons is expect to be better than 90%.

Because the detector is absorbing the energy of the particles, their motion will be affected. Also, because particles must pass through non-active portions of the detector, it is inevitable that they would lose energy to these sections in a way that cannot be as closely measured. Because of this, as well as limitations in the materials in the detector, there will exist inefficiencies in the detection of particles, as well as resolution limitations in the measurements of momentum and energy.

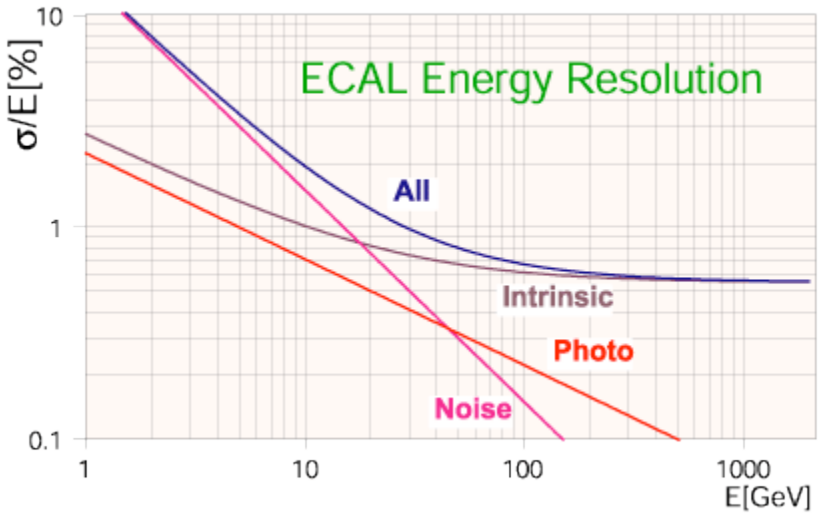


Figure 1.10: The detector has a limit to the accuracy with which it can measure particle energies. Here is the energy resolution for the electromagnetic calorimeter.

However, until these machines turn on, there is no time to waste sitting around. Particle physicists have already started performing calculations that can be included in analyses.

Chapter 2

PYTHIA and Monte Carlo Event Generation

In principle, a collision between two point particles from beams operating at a known center-of-mass energy will give a calculable (see the section on Higgs production and decay) rate for some $2 \rightarrow 2$ process. Because of conservation laws, the momentum is shared equally among the final state particles of the two body interaction in the CM frame. Thus, the final state momenta are equal to the initial state momenta and the decays are isotropic.

However, protons are not the simple point particles described above. The proton has structure, made up of two up quarks and a down quark (three *valence* quarks) bound together by gluons. Furthermore, gluons can pair produce to make virtual quark-antiquark pairs, which can also interact to produce Higgs in a hadron collider. The problem is that the total proton momentum is divided in a non-trivial away among its constituents.

The probability distribution for each constituent (gluon, or sea or valence quark)

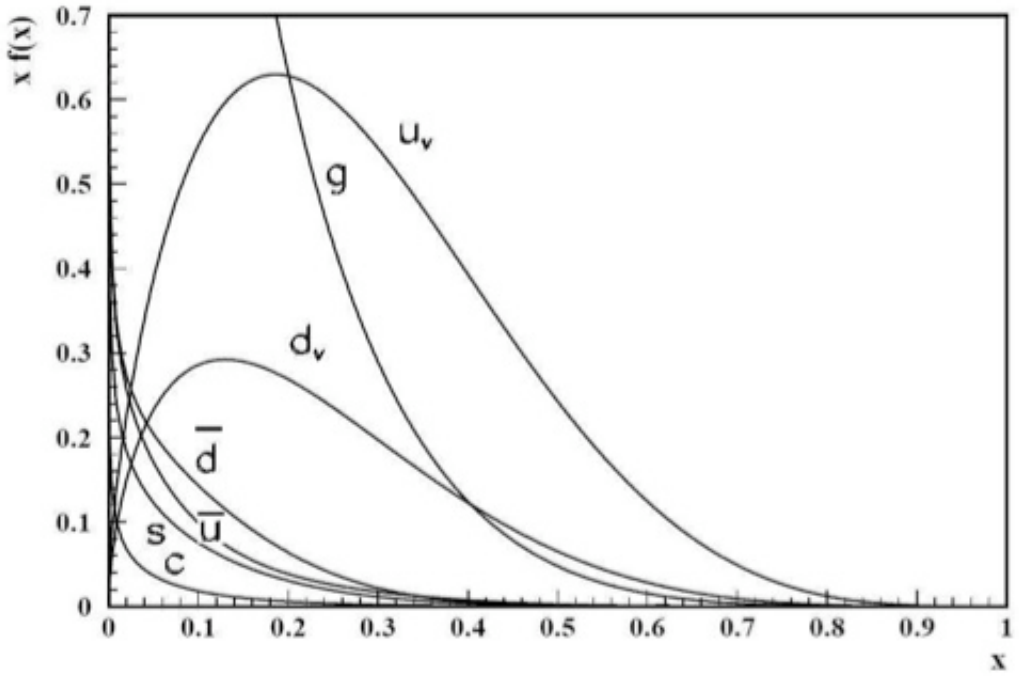


Figure 2.1: The parton distribution function for a proton at $\sqrt{s} = 14$ TeV. x is the fraction of the total momentum, and $f(x)$ is related to the probability for each constituent to carry that fraction. See Reference [6].

to carry a fraction of the total proton momentum is not a calculable function. Instead, the calculation relies on sampling from a *parton distribution function* (PDF), that is derived from data.

By adding this random sampling over initial states, the phase-space integrals involved become too complicated to attempt to solve analytically. The calculation is made by turning to a event generator, called a *Monte Carlo*. Since the LHC and the CMS detector have not been completed yet, no data exists that can be used for analysis. The calculations for Higgs production and decay are complicated and depend on random number generation, so they must be solved numerically. Accordingly, PYTHIA 6.401[4] was used to provide a Monte Carlo calculation of Higgs production at the LHC. A PYTHIA-based program was

subprocess	ISUB	subprocess name
$q_i\bar{q}_i \rightarrow H$	3	
$q_i\bar{q}_i \rightarrow Z^0H$	24	higgsstrahlung (neutral)
$q_i\bar{q}_i \rightarrow W^+H$	26	higgsstrahlung (charged)
$gg \rightarrow H$	102	gluon fusion
$q_i\bar{q}_j \rightarrow q_i\bar{q}_jH$	123	vector boson fusion (neutral)
$q_i\bar{q}_j \rightarrow q_k\bar{q}_lH$	124	vector boson fusion (charged)

Table 2.1: Summary of leading-order Higgs production PYTHIA subprocesses.

subprocess	ISUB
$q_i\bar{q}_i \rightarrow (\gamma^*/Z^0)$	1
$q_i\bar{q}_i \rightarrow (\gamma^*/Z^0)(\gamma^*/Z^0)$	22
$q_i\bar{q}_j \rightarrow (\gamma^*/Z^0)W^+$	23

Table 2.2: Summary of Z background-producing PYTHIA subprocesses.

written to generate event data for $pp \rightarrow H$ at $\sqrt{s} = 14$ TeV. Appendix A gives a fairly standard example of the FORTRAN code written to generate events using PYTHIA. By default, PYTHIA uses SM couplings for the Higgs Boson (`MSTP(4)=0`).

Higgs production at the LHC is simulated by initializing a proton-proton collision at the center-of-mass energy indicated above. Subprocesses for Higgs production could be switched on using the subroutine `MSUB(ISUB)=1` to select desired modes, where `ISUB` is the subprocess identifier. This could also be done for the expected SM Z-producing backgrounds. The relevant PYTHIA subprocesses are summarized in Tables 2.1 and 2.2. Initial state radiation subprocesses, for example $q\bar{q} \rightarrow g(\gamma^*/Z^0)$, are not included explicitly, since they are calculated by PYTHIA during initial state showering routines[1].

For this run, all general switches and parameters were set to their default values,

[1]It is worth noting that PYTHIA falls short in calculating the initial state QCD radiation.

with the exception of the Higgs mass. For example, this parameter could be set to 200 GeV/c^2 by inputting `MSTP(25,4)=200` into the initialization block. Signal events were generated for the Higgs mass at (140, 160, ... , 400 GeV/c^2). Thus, the Higgs production and decay dependencies on the Higgs mass could be explored.

The program that executes a PYTHIA run consists of three main sections; the initialization, the event generation, and the writing of events to file and calculation of the cross section, branching ratios, and other run statistics. Part of the initialization call sets the desired center-of-mass energy, and also sets the number of events that should be generated in a single run. The number of events generated is normalized out of the kinematic distributions during the analysis. Increasing this number just helps improve the statistics of the run.

The number of events should be as high as possible in order to ensure good statistical sampling of the processes. However, due to limitations in disk space, cpu, and time, it is usually necessary to choose a more modest number. Triggers on $E_T > 15$ GeV for electrons and muons are incorporated into the PYTHIA code so that leptons that fail to pass the kinematic cuts are not written to disk. This saves computation time and disk space, similar to how the trigger electronics in the CMS experiment will determine which events to write to disk. In practice, in order to increase statistics, data corresponding to an integrated luminosity of 10 fb^{-1} was generated, and then scaled down to 1 fb^{-1}.

Finally, a data block entry for each particle produced in a single event is written to file. This data block contains information like particle identifiers, as well as the momentum four-vector and production vertex for each particle. An example (abridged) event is printed

($M_H = 200$ GeV/c^2)

subprocess	σ (pb)
$q_i\bar{q}_i \rightarrow H$	3
$q_i\bar{q}_i \rightarrow Z^0H$	24
$q_i\bar{q}_i \rightarrow W^+H$	26
$gg \rightarrow H$	102
$q_i\bar{q}_j \rightarrow q_i\bar{q}_jH$	123
$q_i\bar{q}_j \rightarrow q_k\bar{q}_lH$	124
total H production	9.652
$q_i\bar{q}_i \rightarrow (\gamma^*/Z^0)$	589.8
$q_i\bar{q}_i \rightarrow (\gamma^*/Z^0)(\gamma^*/Z^0)$	11.01
$q_i\bar{q}_j \rightarrow (\gamma^*/Z^0)W^+$	26.92
total Z background	627.7

Table 2.3: PYTHIA-calculated cross sections for Higgs production and SM Z production for $M_H = 200$ GeV/c^2.

out in Appendix B. This is repeated for however many events are requested. To give an idea of the magnitude of these event files, a typical single event will contain more than 1000 particles. Once this file full of events and four-vectors is obtained, the analysis can begin.

Before beginning the analysis, MC-simulated runs were generated for all the processes in Tables 2.1 and 2.2 for various values of the Higgs mass. The statistics represent the generation of 10^4 events with triggering on leptons with $E_T > 15$ GeV/c.

After generating the run statistics, PYTHIA reports values for the cross sections calculated for each production subprocess. These results are summarized for a particular choice of Higgs mass ($M_H = 200$ GeV/c^2) in Table 2.3, along with the total cross sections for the Higgs (signal) production and the Z (background) production[2]. The PYTHIA-calculated cross section for each of the top five Higgs production subroutines at the LHC is plotted in Figure 2.2. Compare this to the NLO calculation is Figure 1.2.

Furthermore, PYTHIA also calculates the branching ratios for each of the Higgs

[2]Note that the SM Z background cross sections do not depend on Higgs mass.

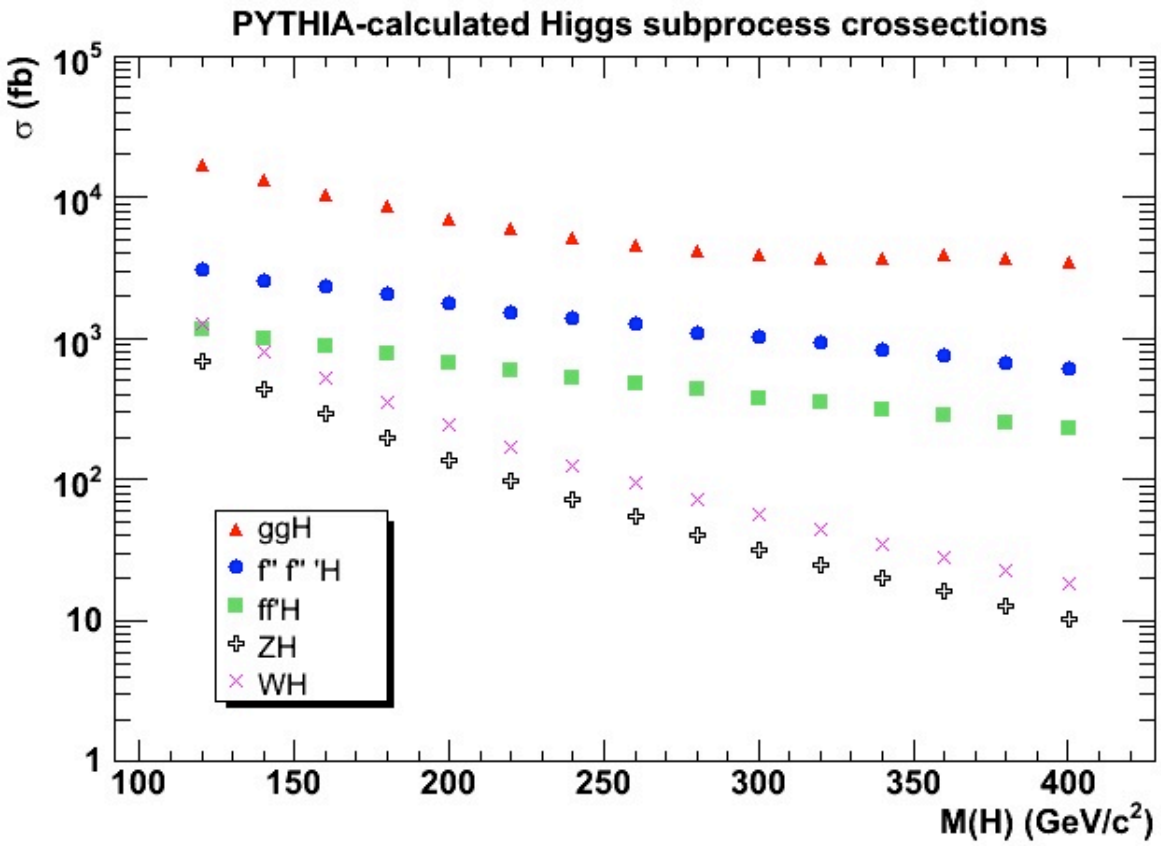


Figure 2.2: PYTHIA-reported cross sections for the five leading production subprocesses for Higgs at the LHC as a function of Higgs mass.

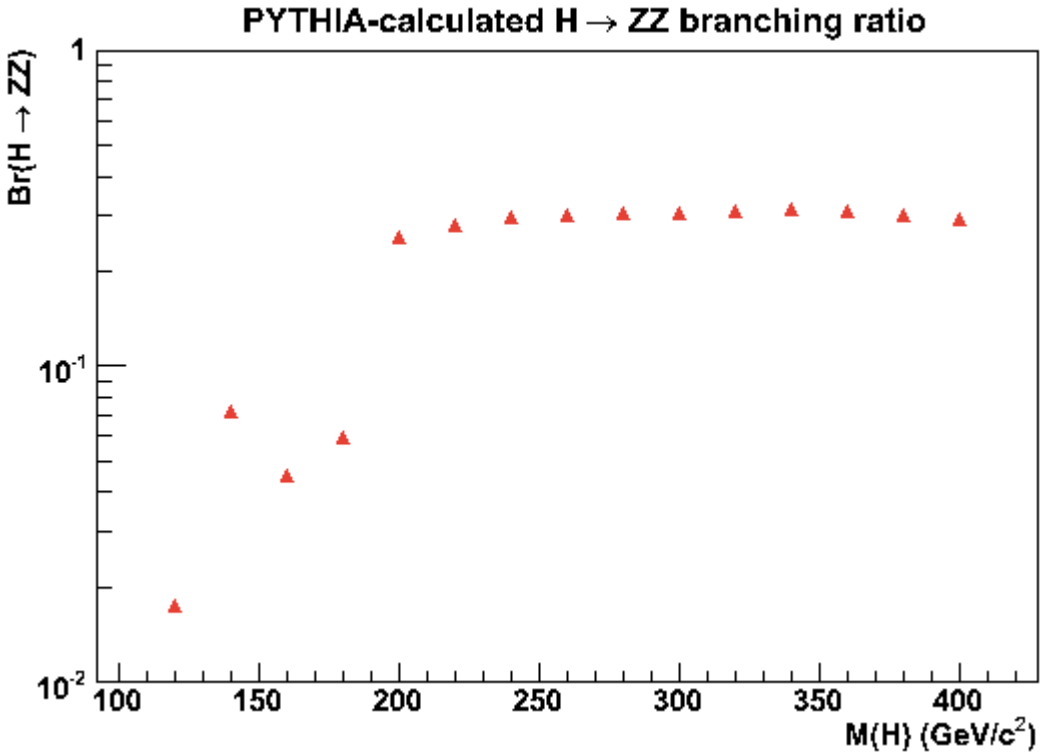


Figure 2.3: PYTHIA-reported branching ratio for H → ZZ as a function of Higgs mass.

decay modes, for each value of the Higgs mass. The most relevant decay channel for the analysis presented here is H → ZZ, which is plotted in Figure 2.3. Again, compare this to the NLO calculation in Figure 1.3.

Once these files are written, they are ready for use in an analysis.

Chapter 3

Analysis and Discussion

In general, particle physics analyses can be quite complicated and intricate. Additional methods can always be used to attempt to improve purity, acceptance, or signal-to-background. However, the more complicated the analysis, the harder it is to make convincing conclusions, and often the physics behind many of the analyses becomes obscured.

The analyses presented here focus on a specific decay channel for the Higgs boson, known as the "Golden Mode" for Higgs discovery at the LHC. This decay channel features the Higgs decay to two Z particles, with each Z then decaying to two leptons. Referring back to the calculated Higgs branching ratios in Figure 1.3, the H $\rightarrow$ ZZ branching ratio varies across the entire expected Higgs mass range. Note that for the low Higgs mass (< 200 GeV/c^2), the branching ratio for H $\rightarrow$ ZZ tends toward zero, since the Higgs is no longer heavy enough to produce two on-shell Z particles. This makes the ZZ analysis difficult at low Higgs mass. However, leptons (electrons and muons) can be measured with reasonably good detection efficiency and resolution in the CMS detector. This makes paying the 3.5%

branching ratio for $Z \rightarrow \ell\bar{\ell}$ worth it.

However, because of the compounded cost of the branching ratios required to fully reconstruct the Higgs from four leptons, it is interesting and perhaps more physically intuitive to try to develop signatures for new physics by studying the kinematics of particle production and decay in a collider experiment rather than fully reconstruct. By studying the kinematics of the Z particles produced from Higgs decays, it may be possible to gain somewhat higher sensitivity for a signal for a lower Higgs mass than is possible with full reconstruction with a large data set.

3.1 Full reconstruction

Full reconstruction involves adding the lepton four-vectors to reconstruct dileptons (Z-candidates), whose four-vectors could then be added together to reconstruct the Higgs from which they decayed. A cartoon of this process is shown in Figure 3.1.

Acceptance cuts of $|\eta| < 2.5$ (*pseudorapitiy*) and $E_T > 25$ GeV were put on all the leptons in the recorded events. The pseudorapidity effectively measures the particle's Lorentz boost in relation to the longitudinal (parallel to the beam pipe) and transverse (into the detector) directions. If the particle has a lot of longitudinal momentum compared to the transverse momentum component (high $|\eta|$), it will simply fly down the beampipe without hitting the detector. Furthermore, the transverse energy cut is used to distinguish the high-energy leptons that decay from a Z particle from other leptons that can be present in an event.

The Z-candidates were reconstructed from all possible lepton pairs, while conserv-

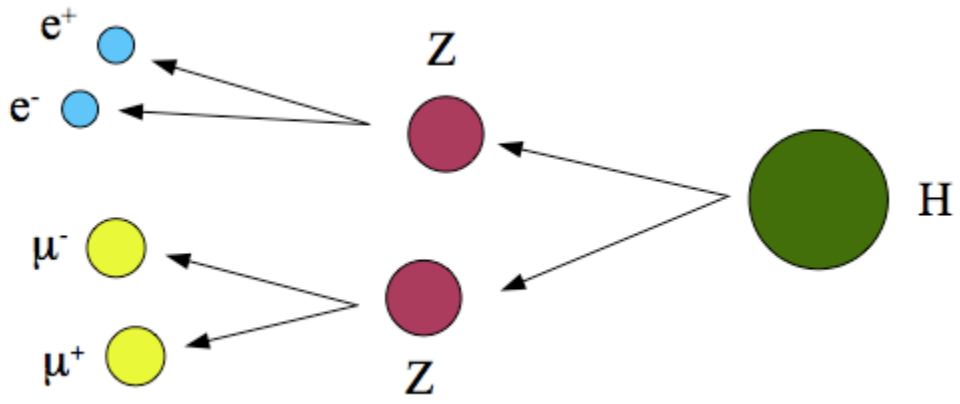


Figure 3.1: A simple cartoon demonstrating the reconstruction of the Higgs from leptons that decayed from ZZ.

ing charge and lepton number, with the intent of building dileptons whose invariant masses were closest to the on-shell Z mass at 91 GeV/c^2. For example, if there were three electrons, the Z was constructed from the two that had an invariant mass closest to 91 GeV/c^2.

Z-candidate pairs (Higgs candidates) were reconstructed from the PYTHIA-generated 10 fb^{-1} event lists. A histogram was made of the invariant mass of the Z-candidate pairs. The histograms were then scaled to an integrated luminosity of 1 fb^{-1}. The results for a Higgs mass of 200 and 400 GeV/c^2 are shown in Figure 3.2.

With 1 fb^{-1}, for a 400 GeV/c^2 Higgs, a clear peak in the total two-Z mass is visible, peaked at the Higgs mass. Although, for the 200 GeV/c^2 Higgs, the signal is still peaked at the Higgs mass, it lies right below the peak for the SM ZZ background. Though a peak is easier to distinguish from background at a higher Higgs mass, the number of Higgs produced starts to fall because of decreasing cross sections. Additionally, the width of the Higgs becomes large. Thus, the peak broadens and flattens considerably at higher mass.

Of course, the detector will not be able to differentiate between signal and back-

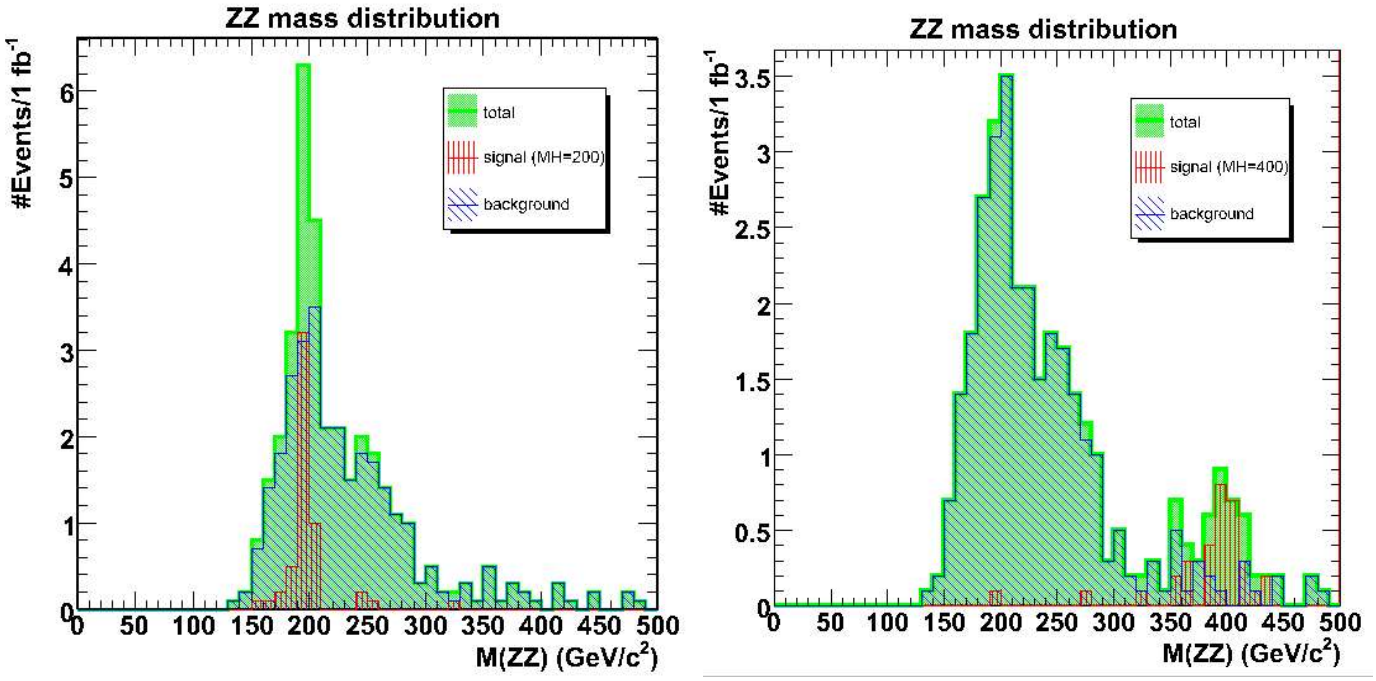


Figure 3.2: Histogram plots of the invariant mass of Z-candidate pairs for various values of the Higgs mass.

ground events, and so it will give the total number of events, the signal plus background. The discovery potential can be quantified by counting the number of observed events and comparing it to the number of expected background events calculated from the Monte Carlo. Since the number of expected events is subject to statistical fluctuations, approximately proportional to the square root of the number of calculated background events, it makes sense to define a significance for the measurement as $\frac{S}{\sqrt{B}}$, where S is the observed number of excess events, and B is the predicted number of background events. A significance of at least 5 (i.e., $S = 5\sqrt{B}$) is needed to make a convincing argument for a new physics.

To make this calculation, the number of events can be counted within a mass window of a width of 10 GeV/c^2. This windowing allows more sensitivity to the fact that the Higgs signal events are sharply peaked. Using this method, a calculation can be made for the significance of the signal as a function of Higgs mass for 1 fb^{-1} using full reconstruction. The result is shown in Figure 3.3. The significance creeps up as the Higgs mass gets higher, approaching a high likelihood of discovery for $M_H > 400$ GeV/c^2.

Generally, this full reconstruction will not make a Higgs discovery with a low-data sample. This is especially true for the low Higgs mass region. The problem is that the full reconstruction is too restrictive. It is worthwhile to look for ways to increase the number of signal events while decreasing the backgrounds. From Figure 3.4, the number of signal events drops drastically as more leptons passing the cuts are required, mostly due to the branching ratios. It may help to increase signal by considering an analysis that loosens these requirements, and then focuses on kinematics unique to the Higgs decay.

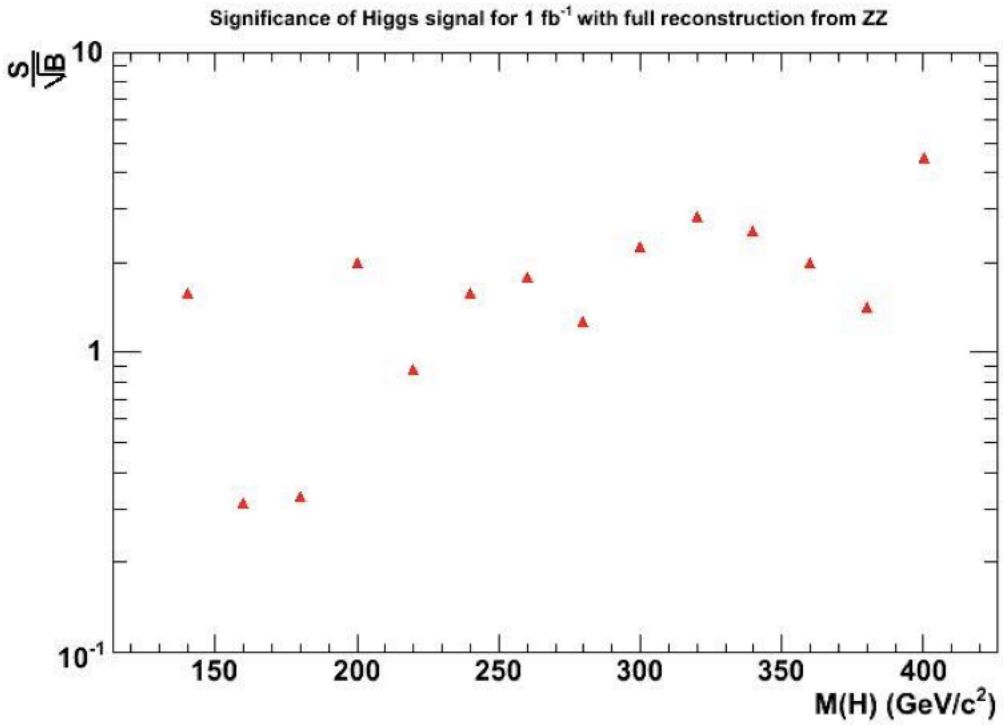


Figure 3.3: The significance of the Higgs signal for 1 fb^{-1} as a function of the Higgs mass for full reconstruction.

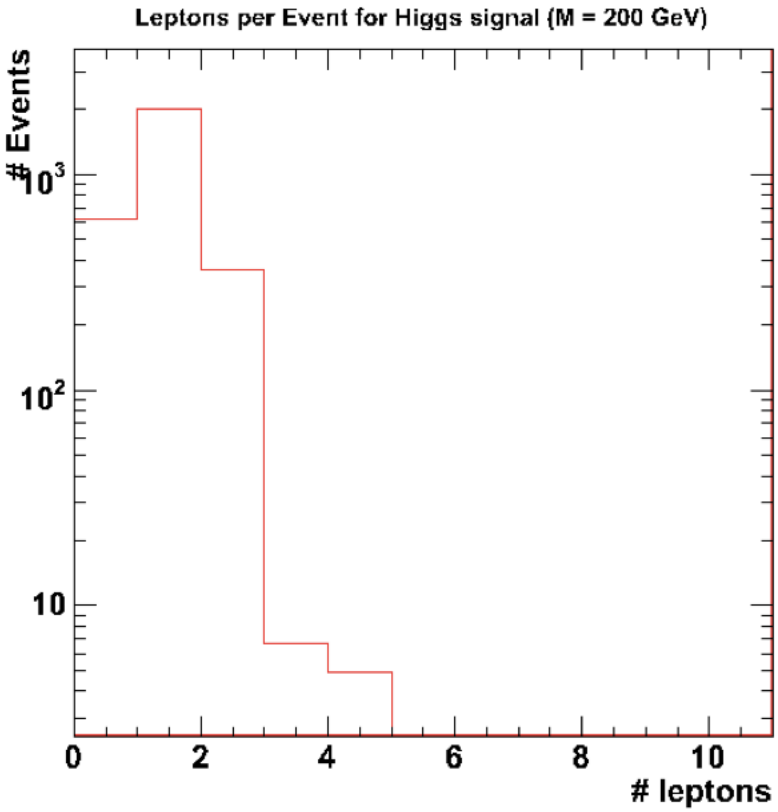


Figure 3.4: A histogram of the number of events with a given number of leptons per event that pass the acceptance cuts, for the signal events.

3.2 Transverse Momentum Signature of a Single Z

Referring to Figure 3.4, it is clear that by requiring only two leptons in an event, the signal will go up considerably. Thus, additional events are gained from cases where the Higgs decays to two Z particles, with one Z decaying to two leptons. The other Z can decay to anything, thus dropping a factor of the $Z \to \ell\bar{\ell}$ branching ratio. (See Figure 3.5) The kinematic cuts on the leptons ($|\eta| < 2.5$ and $E_T > 25$ GeV) are still in place.

However, whatever was gained from this trick has been completely swamped by the single Z background from $pp \to Z$. (See Figure 3.6) Since it is rare for this background to have more than two leptons that pass the kinematic cuts, this background did not show up in the full reconstruction. However, here the cross section for this subprocess is orders of magnitude higher than the total signal cross section. A quick glance at Figure 3.7 sheds some insight into the problem. There are 5×10^5 single Z particles generated in 1 fb^{-1} from this background alone. The ability to extract any meaningful signal evaporates as a result.

3.3 Transverse Momentum of a Z with a Third Lepton

Figure 3.7 suggests that the leading Z background can be dispatched by requiring a third lepton in each event. The signal still takes a significant reduction, but it is worth it for not having to deal with a mountain of additional background. In the case of two Z-candidates in the event (i.e., an event for which both Z decayed to leptons), the lepton pair is chosen with an invariant mass closest to 91 GeV/c^2. The kinematic cuts on the leptons are still in place.

The Z background from the ZZ and WZ subprocesses persists in the p_T(Z) plot

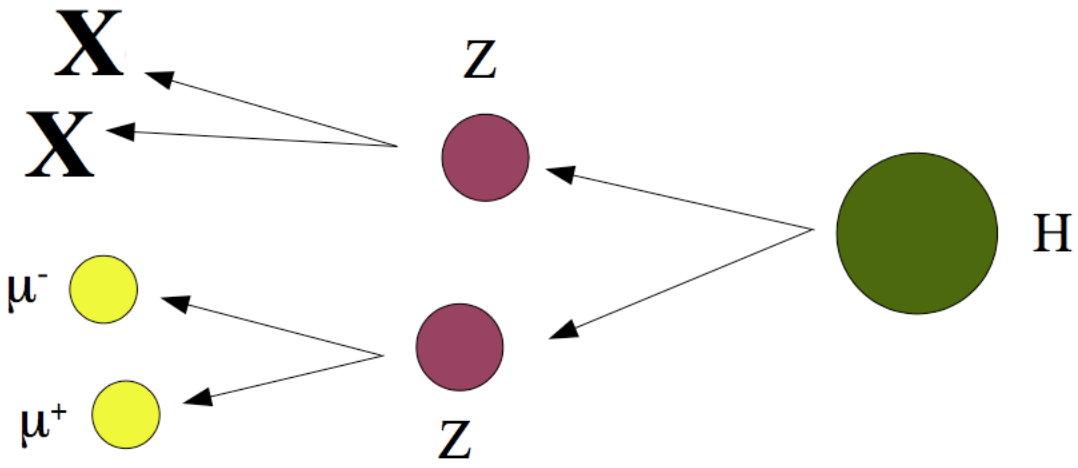


Figure 3.5: Here only one Z-candidate is reconstructed. This increases the total number of observed events.

(Figure 3.8), with a sharp rise at low momentum, and then a long tail to high momentum.

The disadvantage of looking at the transverse momentum is that the signal peak loses its sharpness. Whereas the invariant mass peak of the four-lepton system was a sharp gaussian, the p_T is a much softer shape, peaking at the difference between the Higgs mass and twice the on-shell mass of a Z.[1]

As a result of the softness, the windowing method described in the section on full reconstruction will not work as well here. The significance is plotted in Figure 3.9 as a function of Higgs mass for the p_T(Z) with the presence of a third lepton. Without the windowing, even though there are more signal events they are harder to separate from the background. Despite this, for the low Higgs mass, the significance is a little higher for a signal here than for with the full reconstruction. However, the significance is not high

[1]In the case where this is bigger than the Higgs mass, the distribution peaks approximately at the Higgs mass minus the mass of one on-shell Z. The other Z takes up a little momentum, but is off-shell and so there is no shift from the mass.

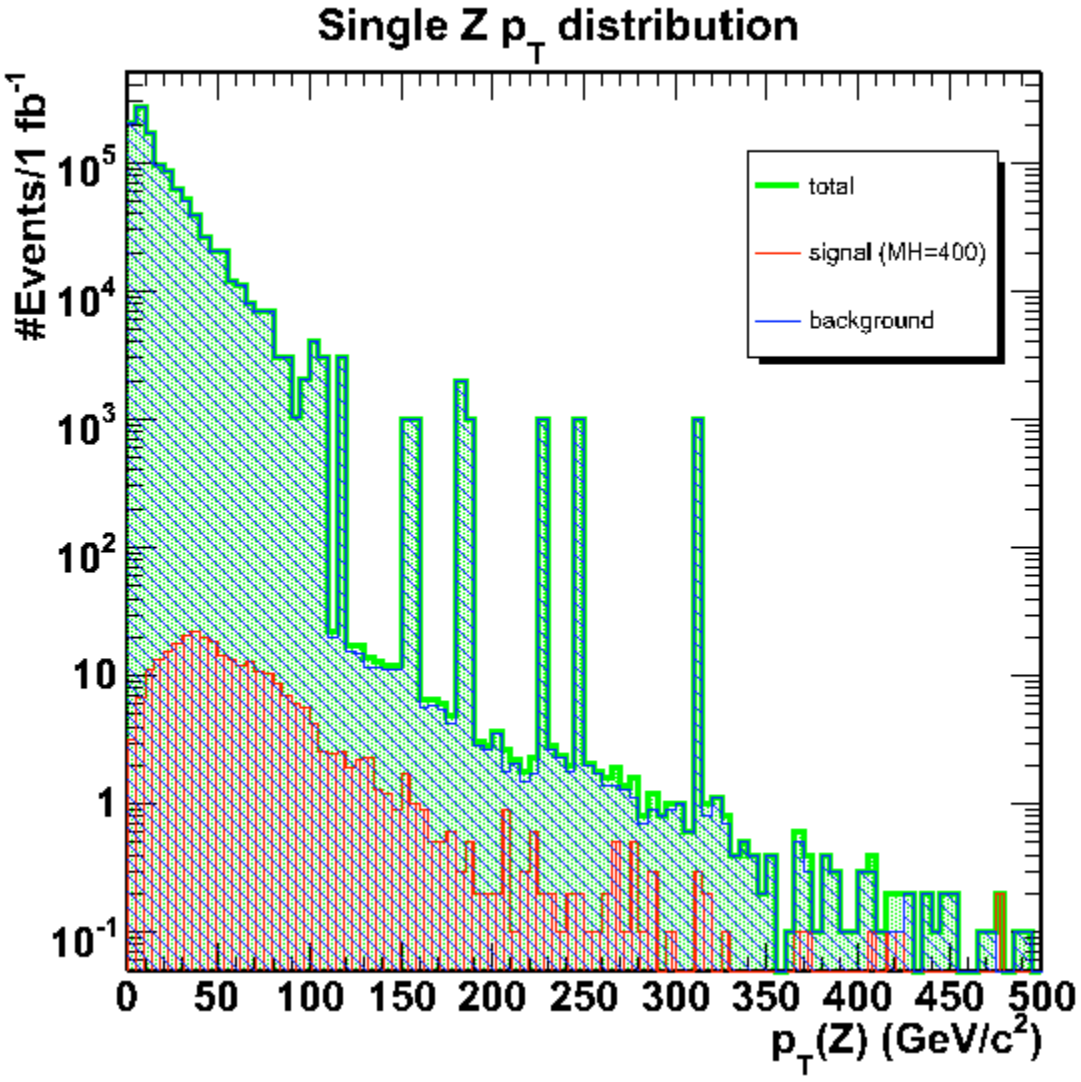


Figure 3.6: The transverse momentum plot of a single Z. Good luck extracting that signal!

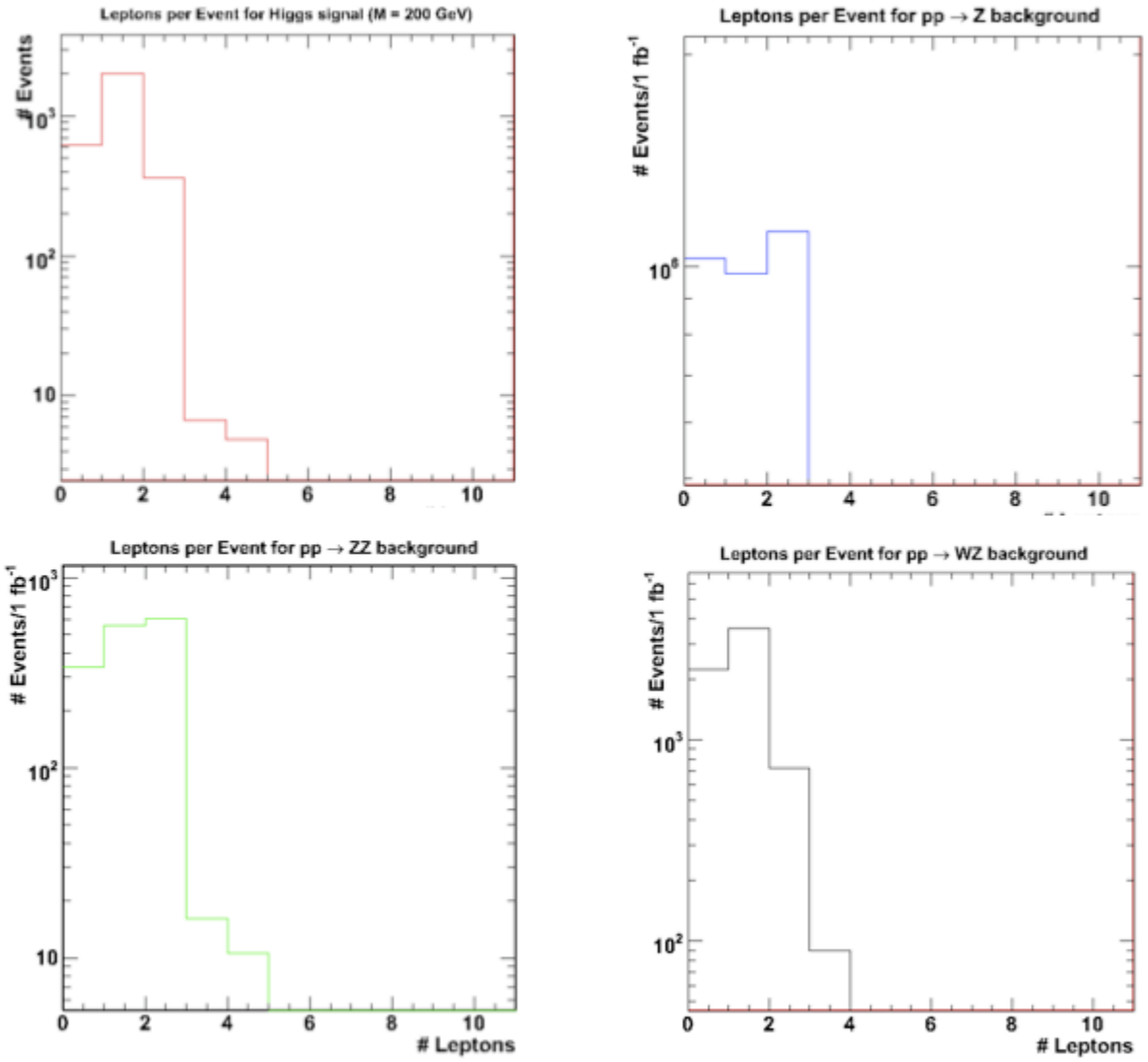


Figure 3.7: A histogram of the number of events with a given number of leptons per event that pass the acceptance cuts

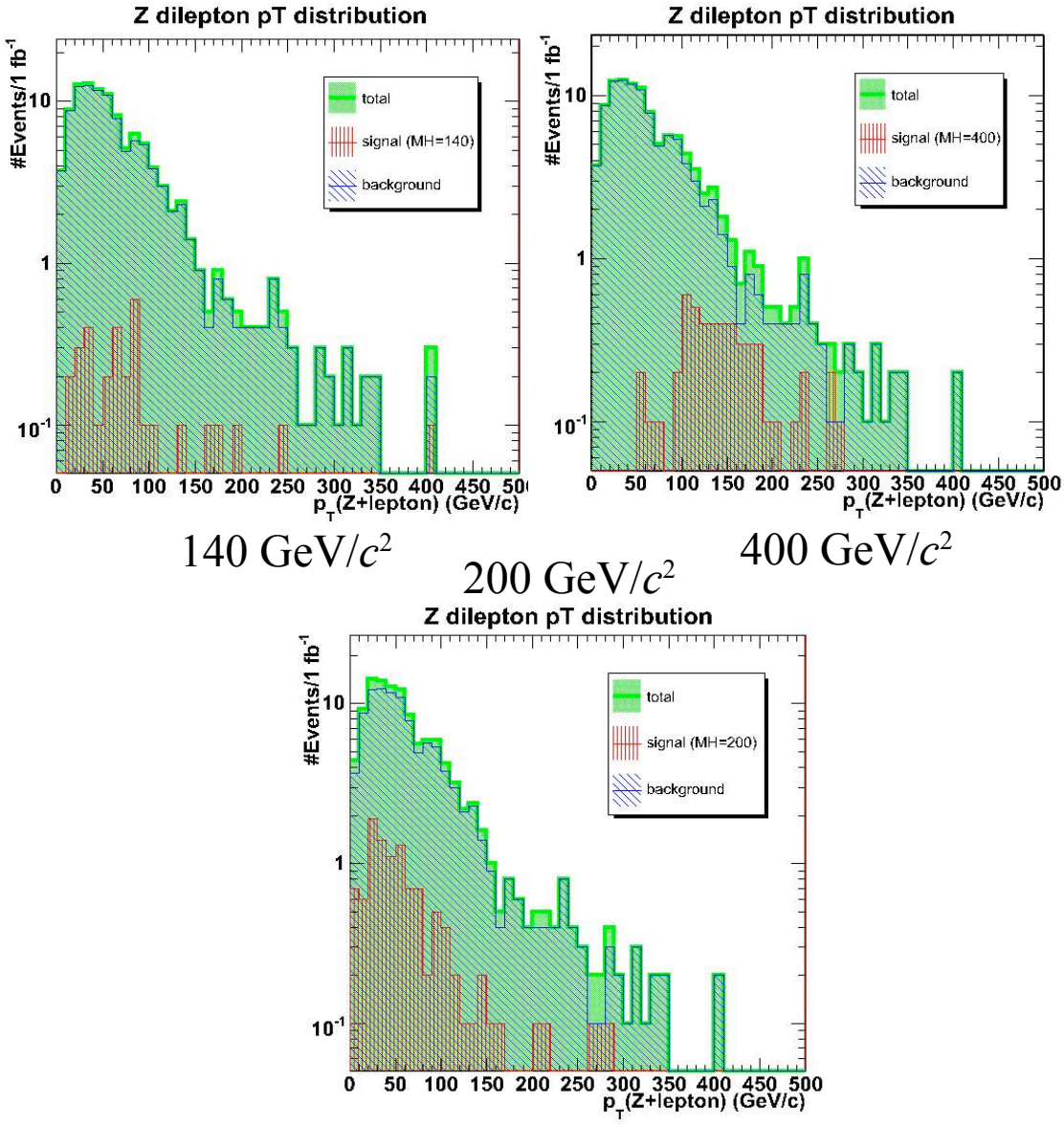


Figure 3.8: The p_T of the single Z (plus a third lepton) for the Higgs daughter and SM background Z particles for a few values of the Higgs mass.

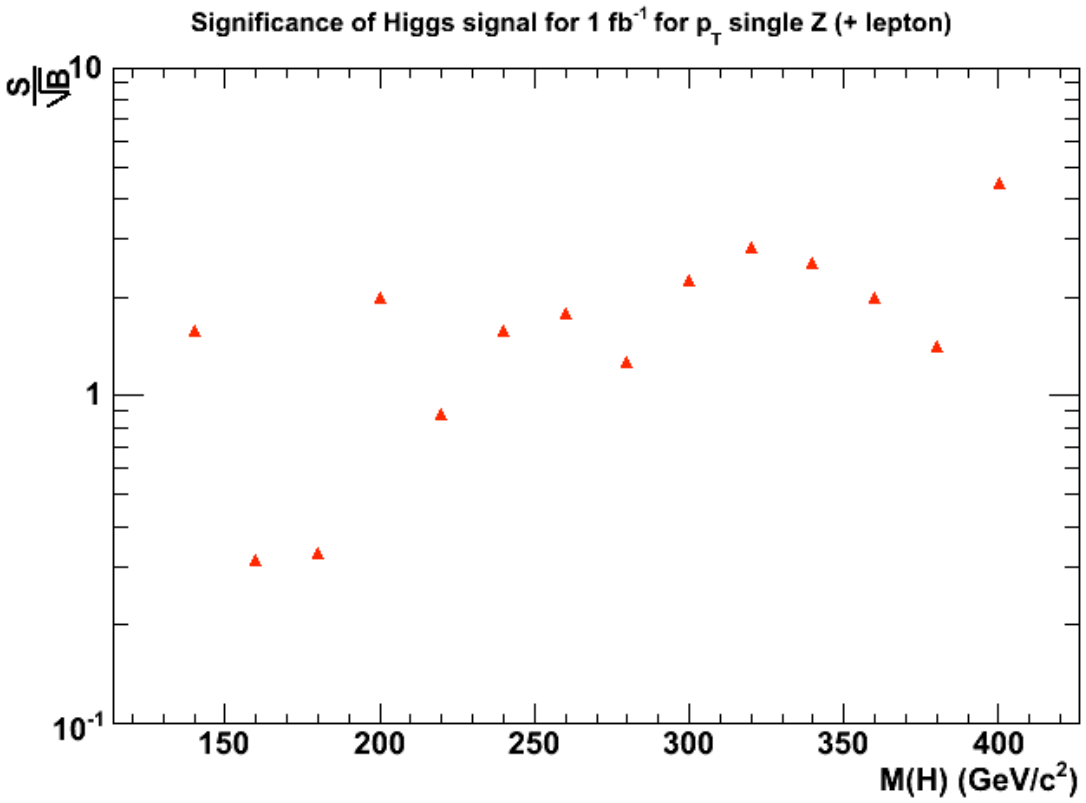


Figure 3.9: The significance of the excess in the transverse momentum of the single Z (plus a third lepton) for a few values of the Higgs mass.

enough for a discovery, and is even lower than full reconstruction for a high mass Higgs.

3.4 Kinematics of a Trilepton System

In order to use this increased signal, as well as take advantage of the unique kinematic distributions, it is interesting to explore the trilepton system. Here, a Z-candiate is found from leptons. A change is made, in that now the Z is required to be on-shell, with a mass between 81 and 101 GeV/c^2. All three leptons must still be within the kinematic cuts as explained above. Now, the third lepton's four-vector is added to that of the Z-candidate,

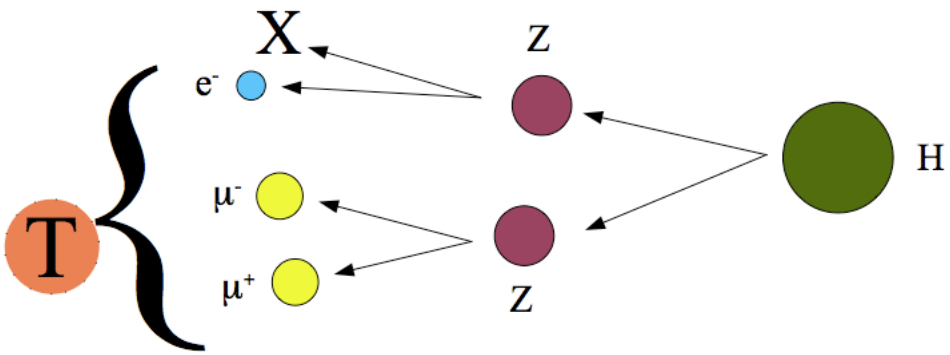


Figure 3.10: The Z-candidate and third lepton are partially reconstructed to form the trilepton.

making an effective trilepton system. (See Figure 3.10)

The trilepton invariant mass can be easily calculated, and in doing so, one derives the nice result (Figure 3.11) that the signal is once again peaked. However, in this case, the background is just as sharply peaked, and even worse, it sits right on top of the signal. The windowing strategy (in 10-GeV/c^2 windows) can be used again, but this still picks up a lot of background.

It is apparent from event counting that using the trilepton signal has given a further edge. There are a few extra signal events from additional Z particles and other high-energy leptons in the event. Mostly, these come from the higgsstrahlung process described before, in which a Higgs is radiated from a virtual W or Z. After the radiation, the W can make a lepton-neutrino pair, or the Z can decay to two leptons, contributing to the total number of leptons, and further increasing the trilepton signal. The smaller peaks to the right of the main peak in the signal in Figure 3.11 are events that come from these processes.

The p_T of the trilepton system is just as easy to calculate. This is shown in Figure 3.13. The transverse momentum distributions have an interesting feature; the background

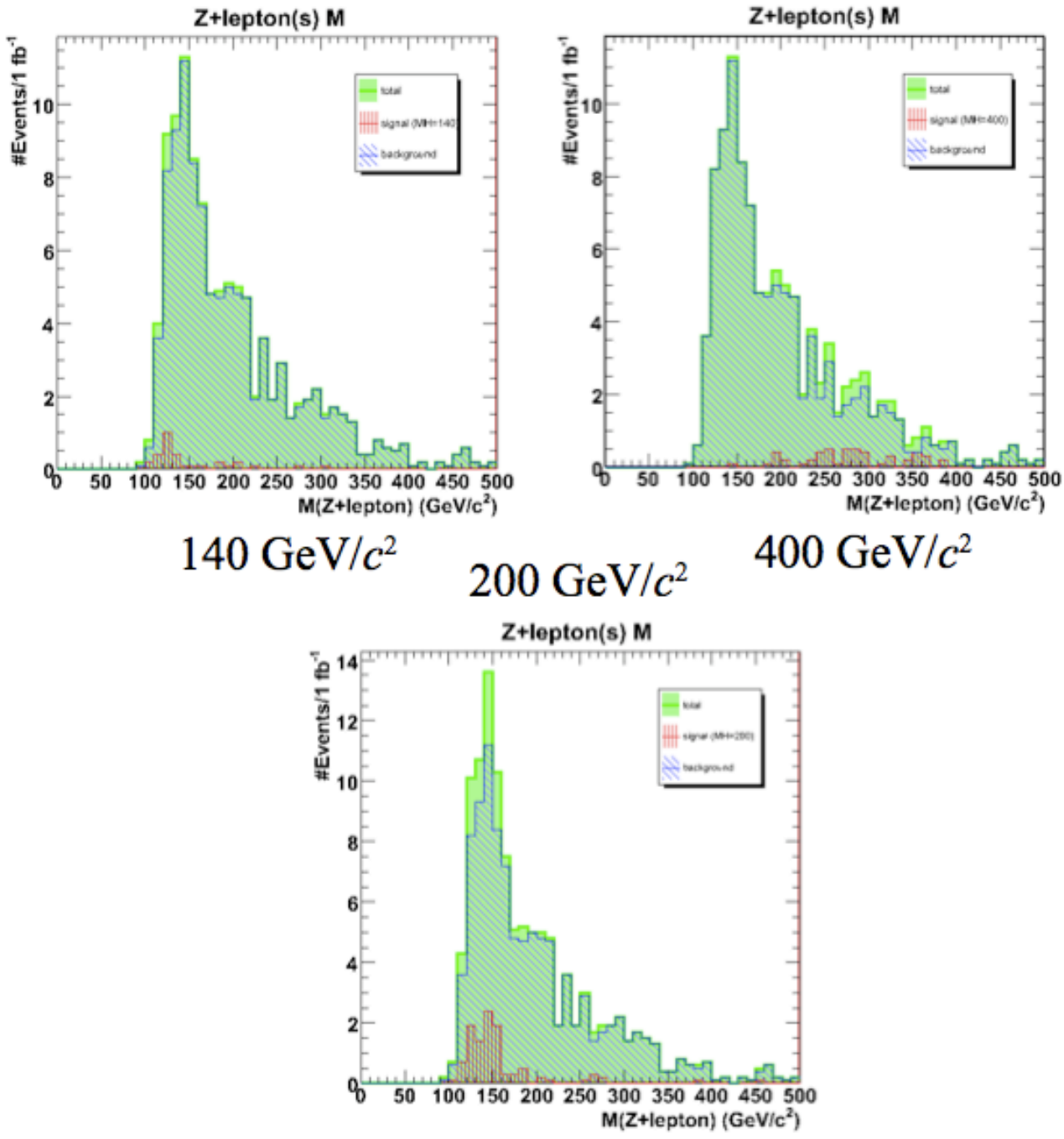


Figure 3.11: Histograms of the trilepton mass, for a few values of the Higgs mass. Again, at higher Higgs mass, the signal peak shifts towards higher mass, but the tail of the background is more overwhelming here.

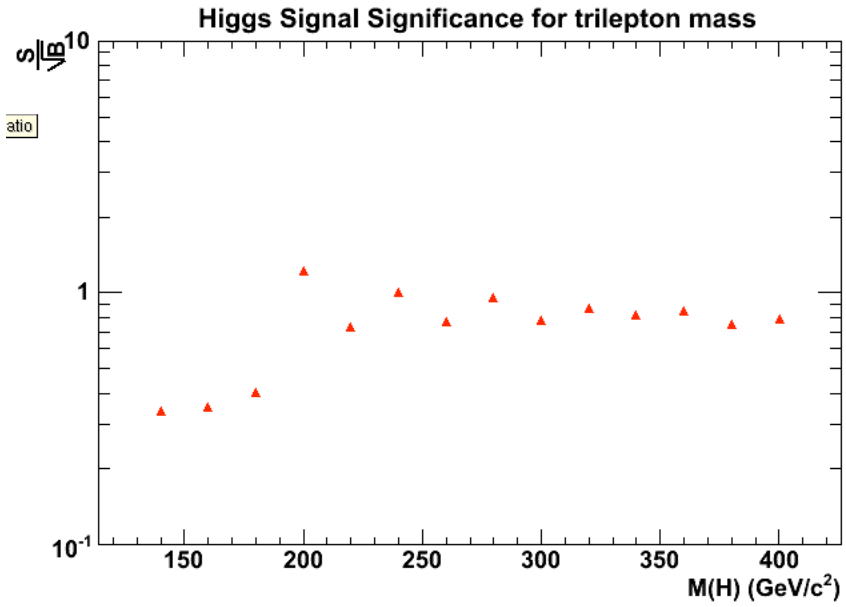


Figure 3.12: The significance of the excess in events for the mass of the trilepton system

peaks tail off to higher p_T, while the signal peaks tail off to lower momentum. However, because of the spreading of the peaks in the distribution, there is no windowing that can eliminate the background, and the events are counted by integrating over the entire range. Because of this, the significance here is the same as for the transverse momentum significance of the single Z (plus lepton), as seen in Figure 3.9.

In either case, consideration of the kinematics of the trilepton system cannot increase the sensitivity further than the analyses already discussed.

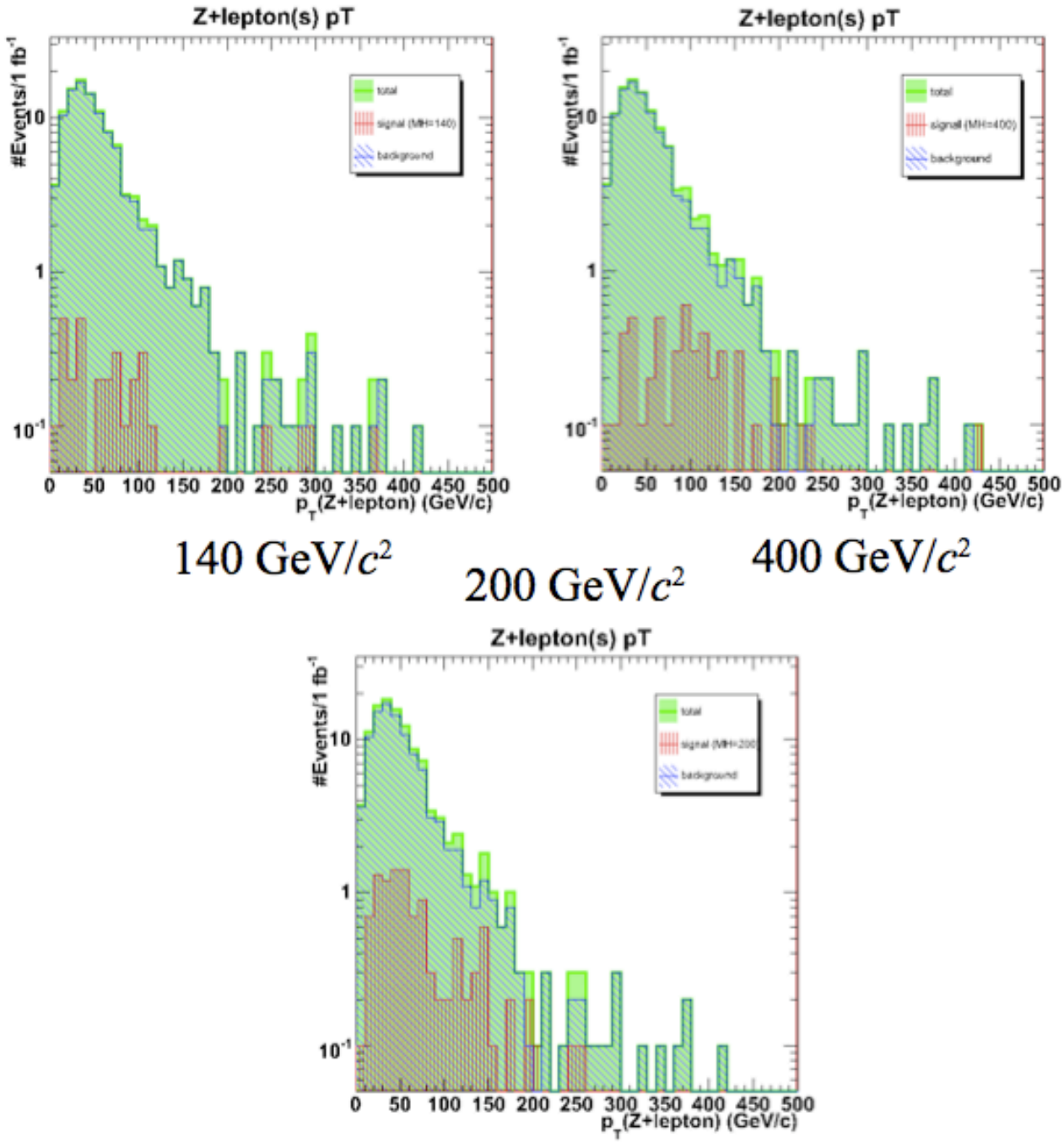


Figure 3.13: Histograms of the trilepton transverse momentum, for a few values of the Higgs mass

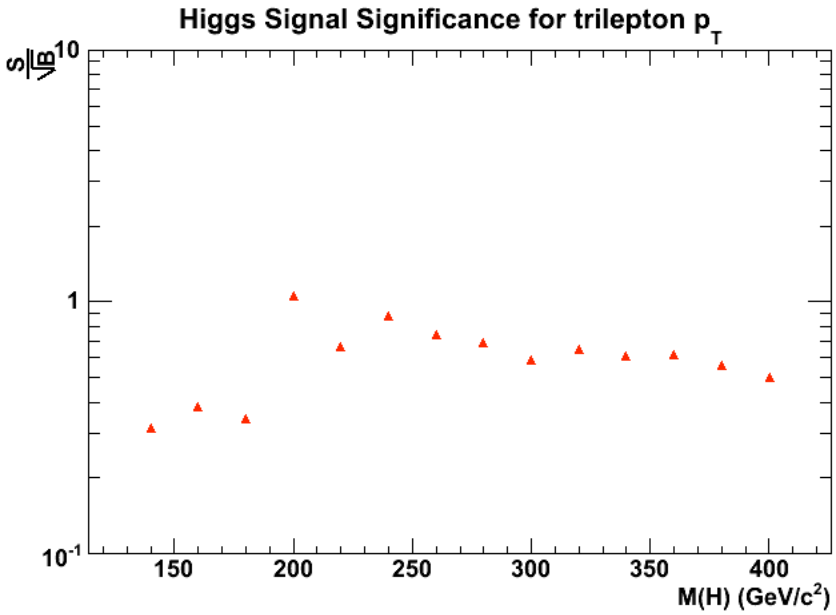


Figure 3.14: The significance of the observed excess in the transverse momentum of the trilepton system

Chapter 4

Conclusion

This paper attempted to explore Higgs discovery potential for the "Golden mode," $pp \rightarrow \mathrm{H} \rightarrow \mathrm{Z}^0\mathrm{Z}^0 \rightarrow \ell\bar{\ell}\ell'\bar{\ell}'$ with analyses other than plotting the invariant mass of the fully reconstructed Higgs. In addition to full reconstruction, this work explored the transverse momentum distributions of a single Z that decayed from the Higgs, as well as the invariant mass and transverse momentum of a trilepton system that decayed from Higgs.

The kinematic analysis presented here was not able to make a significant Higgs boson sensitivity with an integrated luminosity of just 1 fb^{-1}. The significance results are summarized in Figure 4.1. For high Higgs mass ($\mathrm{M}_H > 400$ GeV/c^2), it is clear that full reconstruction has an edge over the partial kinematics explored here. However, it seems that there might be a slight advantage to the kinematic analysis for a low Higgs mass. ($\mathrm{M}_H < 200$ GeV/c^2),

Although no discovery can be made at this level, it should be noted that 1 fb^{-1} only represents a few months' data collection. By simply waiting for more data, the number of

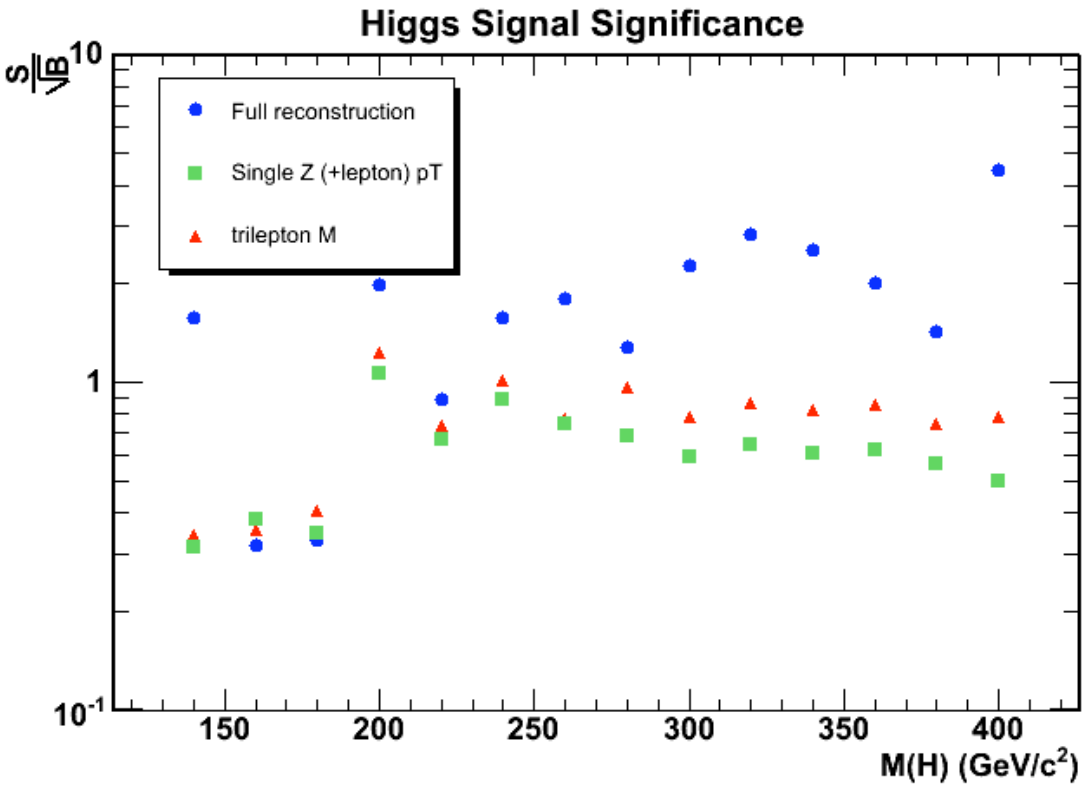


Figure 4.1: All the significances calculated for all the analysis considered in this work.

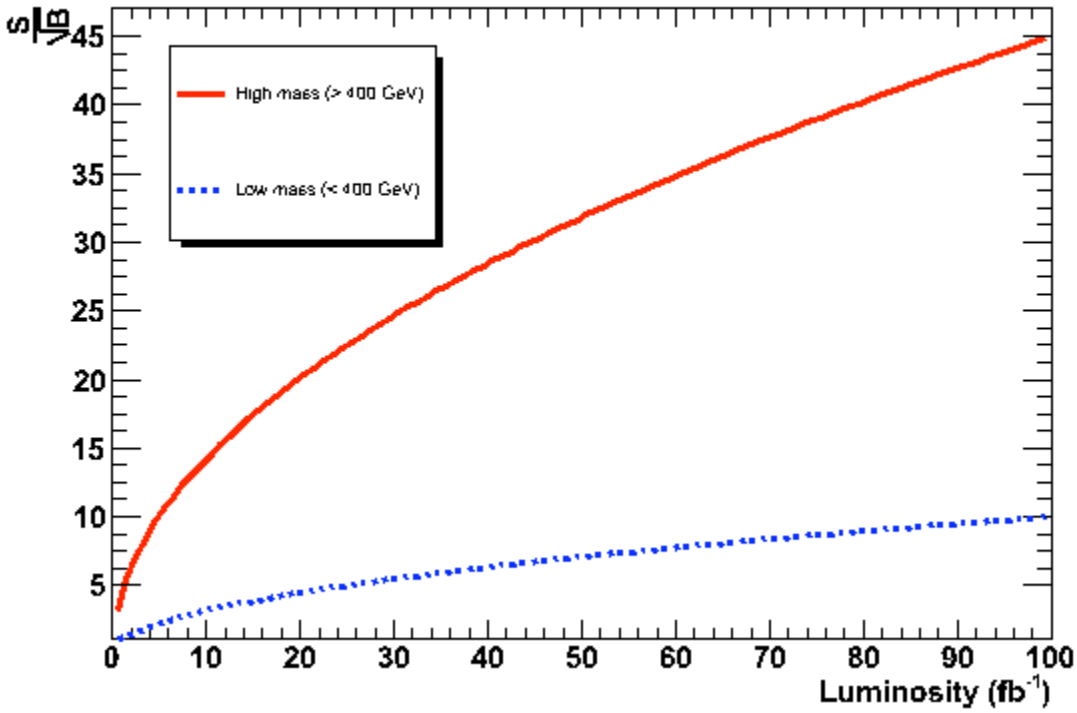


Figure 4.2: The significance for high- and low-mass will scale with the square root of integrated luminosity.

signal and background events should both scale with the integrated luminosity. As a result, the significance should increase with the square root of the integrated luminosity. Making this projection in Figure 4.2, one would need only $\int L\,dt = 1.25$ fb^{-1} to reach a significant signal for a high-mass Higgs ($M_H > 400$ GeV/c^2), but would need 25 fb^{-1} for a low-mass Higgs.

It should be noted that the work presented here ignored a few complications that would go into a full and complete analysis. A perfect detector with 100% efficiency and resolution was assumed. A more sophisticated analysis might use a full simulation of CMS events, not just use generated events as was done here. Furthermore, no account is made of

the rate for hadronic jets to fake leptons. This implies a very high-purity sample. Lastly, since PYTHIA is only a LO Monte Carlo, corrections will have to be made for improper calculation of initial-state QCD radiation effects, and for higher-order diagrams that it simply ignores. The point is, if this analysis is difficult now, these considerations will just make it more difficult. However, by ignoring these effects to first order, it is possible to gain insight into the physics behind the Higgs decays, before bringing in the real-world complications.

This work has presented an analysis that is interesting for at least two reasons; i) it explores the kinematics of Higgs decay in a way that goes beyond the traditional full reconstruction. ii) it may prove to work better than full reconstruction for low-mass Higgs, due to increased sensitivity to this signal and inclusion of events that will not show up in a full reconstruction analysis.

In the end, getting involved in analysis work early will be very useful in preparing for the first run of the LHC. In this exciting time in high energy physics, there may be no telling what happens when particles, and worlds collide.

Bibliography

[1] PW Higgs, PRL **13**, 16 (1964), 508-509

[2] M Spira, Fortsch.Phys. **46**, 3 (1998), 203-284

[3] A Quadt, Higgs Searches at LEP, (2002) hep-ex/0207050

[4] T Sjöstrand *et* al., J. High Energy Phys., (2006) 026

[5] S Eidelman *et* al., Physics Letters B592, 1 (2004)

[6] A Martin *et* al., Phys.Lett. B443 (1998) 301-307

Appendix A

PYTHIA code

```
C...A simple skeleton program, illustrating a typical Pythia run:

C...Preamble: declarations.

C...All real arithmetic in double precision.
      IMPLICIT DOUBLE PRECISION(A-H, O-Z)
C...Three Pythia functions return integers, so need declaring.
      INTEGER PYK,PYCHGE,PYCOMP
C...Parameter statement to help give large particle numbers
C...(left- and righthanded SUSY, excited fermions).
      PARAMETER (KSUSY1=1000000,KSUSY2=2000000,KEXCIT=4000000)

C...EXTERNAL statement links PYDATA on most machines.
      EXTERNAL PYDATA

C...Commonblocks.
C...The event record.
      COMMON/PYJETS/N,NPAD,K(4000,5),P(4000,5),V(4000,5)
C...Parameters.
      COMMON/PYDAT1/MSTU(200),PARU(200),MSTJ(200),PARJ(200)
C...Particle properties + some flavour parameters.
      COMMON/PYDAT2/KCHG(500,4),PMAS(500,4),PARF(2000),VCKM(4,4)
C...Decay information.
      COMMON/PYDAT3/MDCY(500,3),MDME(4000,2),BRAT(4000),KFDP(4000,5)
C...Selection of hard scattering subprocesses.
      COMMON/PYSUBS/MSEL,MSELPD,MSUB(500),KFIN(2,-40:40),CKIN(200)
```

```
C...Parameters.
      COMMON/PYPARS/MSTP(200),PARP(200),MSTI(200),PARI(200)
C...Supersymmetry parameters.
      COMMON/PYMSSM/IMSS(0:99),RMSS(0:99)
C...HEPEVT commonblock.
      PARAMETER (NMXHEP=4000)
      COMMON/HEPEVT/NEVHEP,NHEP,ISTHEP(NMXHEP),IDHEP(NMXHEP),
     &JMOHEP(2,NMXHEP),JDAHEP(2,NMXHEP),PHEP(5,NMXHEP),VHEP(4,NMXHEP)
      DOUBLE PRECISION PHEP,VHEP

C     File logical unit number for output.
      INTEGER LUN
  LUN = 1

      ECM=1000.*14.000D0
      NEV=10000

C     Set the higgs mass
  PMAS(25,1) = 200.

C     Set the process
      MSEL=16
CC     ffbar to Z
C      MSUB(1)=1
CC     Only produce the Z, not the gamma, contribution
C      MSTP(43)=2
C     ffbar to ZZ
C      MSUB(16)=1
C      MSUB(17)=1
C      MSUB(18)=1

C     Initialize.
      CALL PYINIT('CMS','p','p',ECM)

C     Dump the decay table to check that Z0 decay channels set correctly.
      CALL PYSTAT(2)

C       Event loop.
        DO 200 IEV=1,NEV

C         Let pythia generate the event
          CALL PYEVNT

C         List first few events.
```

```
          IF(IEV.LE.4) CALL PYLIST(1)

C         Display an occasional progress update
          IF(MOD(IEV,1000).EQ.0) WRITE(*,*) "Event ",IEV

C         Write this event's information to the dump file so I can
C         later read it into an analysis program (C++ rather than Fortran).

C         First convert the pythia common block to a HEPEVT common
          CALL PYHEPC(1)

C         Determine if the event passes cuts.
C         These cuts only look at the hard scatter part of the event
C         (documentation lines from first 50 lines) to speed to program.
          ITRIG = 0
          MAXL = NHEP
          IF (MAXL .GT. 50) MAXL = 50
          DO 98 IPL=1,MAXL
            IF (ISTHEP(IPL).EQ.3) THEN
              IF (abs(IDHEP(IPL)) .EQ. 11) THEN
                IF (sqrt(PHEP(1,IPL)**2 + PHEP(2,IPL)**2) .GT. 15.) THEN
                  ITRIG=1
                ENDIF
              ENDIF
            ENDIF
   98     CONTINUE

C         Also require a high pT Z
          IHIPTZ=0
          MAXL = NHEP
          IF (MAXL .GT. 50) MAXL = 50
       DO 99 IPL=1,NHEP
         IF (ISTHEP(IPL).EQ.3) THEN
               IF (abs(IDHEP(IPL)) .EQ. 23) THEN
                 IF (sqrt(PHEP(1,IPL)**2 + PHEP(2,IPL)**2) .GT. 80.) THEN
                   IHIPTZ=1
         ENDIF
           ENDIF
         ENDIF
   99     CONTINUE

C         Require both a trigger and a high pT Z
C          IPASS = ITRIG*IHIPTZ
C          IPASS = ITRIG
```

```
C         Use the following line to force all events to pass, if desired.
  IPASS = 1

C         Now write information about all the particles
          MAXWRITE = 40
          IF (IPASS .EQ. 1) THEN
           NLOOP = NHEP
           IF (NLOOP .GT. MAXWRITE) NLOOP = MAXWRITE
           WRITE(LUN,*) '%Evt', NLOOP
           DO 201 IPL=1,NLOOP
C          The ID and three momentum
             WRITE(LUN,*) IDHEP(IPL),PHEP(1,IPL),PHEP(2,IPL),PHEP(3,IPL)
         WRITE(LUN,*) PHEP(4,IPL),PHEP(5,IPL)
C            The status code, parent's index, and first and last
C            daughters' index
             WRITE(LUN,*) ISTHEP(IPL),JMOHEP(1,IPL)
         IF (ISTHEP(IPL).EQ.2)
     &         WRITE(LUN,*) JDAHEP(1,IPL),JDAHEP(2,IPL)
C          The production vertex
             WRITE(LUN,*) VHEP(1,IPL),VHEP(2,IPL),VHEP(3,IPL)
  201      CONTINUE
 ENDIF

C         PYEDIT removes unwanted particles and partons.
C         I don't use it in order to keep the full list.
C         But, I leave it hear for future reference.
C         CALL PYEDIT(3)

C         End event loop.
  200   CONTINUE

C     Write cross section table.
      CALL PYSTAT(1)

C     Signify end of ascii data file
      WRITE(LUN,*) 'exit'

      END
```

Appendix B

A typical PYTHIA event dump

Event listing (summary)

I	particle/jet	KS	KF	orig	p_x	p_y	p_z	E	m
1	!p+!	21	2212	0	0.000	0.000	7000.000	7000.000	0.938
2	!p+!	21	2212	0	0.000	0.000	-7000.000	7000.000	0.938
3	!g!	21	21	1	2.725	1.495	829.316	829.322	0.000
4	!g!	21	21	2	0.117	-0.130	-734.061	734.061	0.000
5	!g!	21	21	3	-0.225	25.547	5.492	26.131	0.000
6	!g!	21	21	4	1.423	-0.060	-632.506	632.508	0.000
7	!h0!	21	25	0	1.198	25.486	-627.014	658.639	200.020
8	!Z0!	21	23	7	41.132	33.865	-361.503	376.703	91.555
9	!Z0!	21	23	7	-39.934	-8.379	-265.511	281.936	85.597
10	!e-!	21	11	8	38.080	25.019	-364.141	366.980	0.001
11	!e+!	21	-11	8	3.052	8.846	2.638	9.723	0.001
12	!e-!	21	11	9	-8.976	-14.478	-2.711	17.249	0.001
13	!e+!	21	-11	9	-30.958	6.099	-262.800	264.687	0.001
14	(h0)	11	25	7	1.198	25.486	-627.014	658.639	200.020
15	(Z0)	11	23	8	41.132	33.865	-361.503	376.703	91.555
16	(Z0)	11	23	9	-39.934	-8.379	-265.511	281.936	85.597
17	e-	1	11	12	-8.976	-14.478	-2.711	17.249	0.001
18	e+	1	-11	13	-30.958	6.099	-262.800	264.687	0.001
19	e-	1	11	10	24.662	16.203	-235.833	237.672	0.001
20	gamma	1	22	10	13.418	8.815	-128.308	129.309	0.000

21	e+		1	-11	11	3.052	8.845	2.637	9.722	0.001
22	gamma		1	22	11	0.000	0.001	0.001	0.001	0.000
23	(u)	A	12	2	3	16.287	-12.787	95.055	97.285	0.330
24	(g)	I	12	21	3	-4.504	-5.195	72.275	72.601	0.000
25	(g)	I	12	21	3	2.066	-5.122	47.477	47.797	0.000
26	(g)	I	12	21	3	1.675	-0.518	19.434	19.513	0.000
27	(g)	I	12	21	3	-0.191	-0.472	6.166	6.187	0.000
28	(g)	I	12	21	3	-3.187	3.324	-12.589	13.404	0.000
29	(g)	I	12	21	3	-1.487	0.182	-4.952	5.174	0.000
30	(g)	I	12	21	3	-1.010	0.269	-3.826	3.966	0.000
31	(g)	I	12	21	3	-7.498	-3.775	-43.055	43.866	0.000
32	(g)	I	12	21	0	-0.813	6.269	-0.567	6.347	0.000
33	(g)	I	12	21	0	-0.372	2.662	-1.867	3.273	0.000
34	(g)	I	12	21	0	1.958	-0.873	0.783	2.283	0.000
35	(g)	I	12	21	0	7.628	-0.256	9.787	12.411	0.000
36	(g)	I	12	21	0	2.463	0.133	4.012	4.710	0.000
37	(g)	I	12	21	0	5.613	2.089	8.079	10.057	0.000
38	(g)	I	12	21	0	8.279	3.766	24.079	25.739	0.000
39	(g)	I	12	21	0	3.332	1.041	11.149	11.683	0.000
40	(g)	I	12	21	0	1.659	0.188	5.657	5.899	0.000
41	(g)	I	12	21	0	3.541	0.454	13.603	14.063	0.000
42	(g)	I	12	21	0	3.154	0.798	24.848	25.061	0.000
43	(g)	I	12	21	0	1.249	0.083	9.035	9.121	0.000
44	(g)	I	12	21	0	13.854	-2.352	163.720	164.322	0.000
45	(g)	I	12	21	0	1.016	-0.838	20.354	20.396	0.000
46	(g)	I	12	21	0	0.813	-6.269	85.194	85.428	0.000
47	(g)	I	12	21	0	-5.351	-5.783	478.328	478.393	0.000
48	(g)	I	12	21	0	-1.016	0.838	58.892	58.907	0.000
49	(g)	I	12	21	0	-2.853	0.655	172.330	172.355	0.000
50	(g)	I	12	21	0	-7.628	0.256	321.697	321.787	0.000
51	(g)	I	12	21	0	-2.463	-0.133	84.888	84.924	0.000
52	(g)	I	12	21	0	-2.034	-0.078	51.229	51.269	0.000
53	(g)	I	12	21	0	-1.249	-0.083	22.942	22.976	0.000
54	(g)	I	12	21	0	-3.491	4.454	14.499	15.564	0.000
55	(g)	I	12	21	0	-3.154	-0.798	12.169	12.597	0.000
56	(g)	I	12	21	0	0.007	-1.057	3.206	3.376	0.000
57	(g)	I	12	21	0	-3.083	-9.074	18.237	20.601	0.000
58	(g)	I	12	21	0	-2.420	-3.134	3.771	5.468	0.000
59	(g)	I	12	21	0	-5.989	-6.079	3.412	9.191	0.000
60	(g)	I	12	21	0	-1.184	-3.513	1.424	3.972	0.000
61	(g)	I	12	21	0	-0.344	-1.068	-0.068	1.125	0.000
62	(g)	I	12	21	0	3.491	-4.454	-0.662	5.698	0.000
63	(g)	I	12	21	0	3.617	-2.132	-6.618	7.837	0.000
64	(g)	I	12	21	0	1.666	0.391	-5.960	6.201	0.000

65	(g)	I	12	21	0	5.351	5.783	-15.065	17.002	0.000
66	(g)	I	12	21	0	0.553	2.278	-3.758	4.430	0.000
67	(g)	I	12	21	0	0.706	2.574	-14.221	14.469	0.000
68	(g)	I	12	21	0	3.025	6.451	-37.798	38.464	0.000
69	(g)	I	12	21	0	5.989	6.079	-68.464	68.994	0.000
70	(g)	I	12	21	0	1.184	3.513	-49.462	49.600	0.000
71	(g)	I	12	21	0	0.408	2.268	-34.194	34.271	0.000
72	(g)	I	12	21	0	0.928	5.555	-147.860	147.967	0.000
73	(g)	I	12	21	0	2.633	1.312	-162.725	162.751	0.000
74	(g)	I	12	21	0	0.279	0.011	-23.887	23.889	0.000
75	(g)	I	12	21	0	-0.102	1.355	-313.444	313.447	0.000
76	(ud_0)	V	11	2101	2	0.277	0.010	-2813.044	2813.044	0.579
77	(ubar)	A	12	-2	3	0.272	-1.306	5.107	5.289	0.330
78	(u)	V	11	2	1	-1.470	-0.226	60.372	60.391	0.330
79	(s)	A	12	3	0	5.140	-2.249	25.927	26.527	0.000
80	(g)	I	12	21	0	1.391	3.552	7.092	8.053	0.000
81	(g)	I	12	21	0	-1.253	1.682	1.439	2.544	0.000
82	(g)	I	12	21	0	-1.060	0.843	0.084	1.357	0.000
83	(g)	I	12	21	0	-1.659	-0.188	0.437	1.726	0.000
84	(g)	I	12	21	0	-0.279	-0.011	0.303	0.412	0.000
85	(sbar)	V	11	-3	0	-5.140	2.249	4.052	6.920	0.000
86	(d)	A	12	1	0	-2.608	-4.886	-230.068	230.134	0.000
...										
1147	gamma		1	22	1025	-0.095	0.059	-0.062	0.128	0.000
1148	gamma		1	22	1026	-0.006	0.008	-0.002	0.010	0.000
1149	gamma		1	22	1026	0.091	-0.223	-0.778	0.815	0.000
1150	pi+		1	211	1027	-0.719	0.434	-3.691	3.788	0.140
1151	pi-		1	-211	1027	-0.446	0.145	-1.158	1.257	0.140
1152	gamma		1	22	1105	0.012	0.089	-0.102	0.136	0.000
1153	gamma		1	22	1105	-0.039	-0.021	0.007	0.045	0.000
1154	pi-		1	-211	1109	-0.243	-0.131	-0.764	0.824	0.140
1155	pi+		1	211	1109	0.105	-0.036	-1.210	1.223	0.140
		sum:		2.00		0.00	0.00	0.00	14000.00	14000.00